



## Seasonality of ecosystem respiration and gross primary production as derived from fluxnet measurements

Eva Falge<sup>a,\*</sup>, Dennis Baldocchi<sup>b</sup>, John Tenhunen<sup>a</sup>, Marc Aubinet<sup>c</sup>, Peter Bakwin<sup>d</sup>, Paul Berbigier<sup>e</sup>, Christian Bernhofer<sup>f</sup>, George Burba<sup>g</sup>, Robert Clement<sup>h</sup>, Kenneth J. Davis<sup>i</sup>, Jan A. Elbers<sup>j</sup>, Allen H. Goldstein<sup>b</sup>, Achim Grelle<sup>k</sup>, André Granier<sup>l</sup>, Jón Guðmundsson<sup>m</sup>, David Hollinger<sup>n</sup>, Andrew S. Kowalski<sup>o</sup>, Gabriel Katul<sup>p</sup>, Beverly E. Law<sup>q</sup>, Yadvinder Malhi<sup>h</sup>, Tilden Meyers<sup>r</sup>, Russell K. Monson<sup>s</sup>, J. William Munger<sup>t</sup>, Walt Oechel<sup>u</sup>, Kyaw Tha Paw U<sup>v</sup>, Kim Pilegaard<sup>w</sup>, Üllar Rannik<sup>x</sup>, Corinna Rebmann<sup>y</sup>, Andrew Suyker<sup>g</sup>, Riccardo Valentini<sup>z</sup>, Kell Wilson<sup>r</sup>, Steve Wofsy<sup>t</sup>

<sup>a</sup> Pflanzenökologie, Universität Bayreuth, 95440 Bayreuth, Germany

<sup>b</sup> ESPM, University of California at Berkeley, Berkeley, CA 94720, USA

<sup>c</sup> Unité de Physique, Faculté des Sciences, Agronomiques de Gembloux, B-50 30 Gembloux, Belgium

<sup>d</sup> NOAA/OAR, Climate Monitoring and Diagnostics Laboratory, 325 Broadway, Boulder, CO 80303, USA

<sup>e</sup> INRA, Bioclimatologie, Bordeaux, France

<sup>f</sup> Technische Universität Dresden, IHM Meteorologie, Piennner Str. 9, 01737 Tharandt, Germany

<sup>g</sup> School of Natural Resource Sciences, University of Nebraska-Lincoln, 244 L.W. Chase Hall, P.O. Box 830728, Lincoln, NE 68583-0728, USA

<sup>h</sup> Institute of Ecology and Resource Management, University of Edinburgh, Edinburgh EH9 3JU, UK

<sup>i</sup> Department of Meteorology, Pennsylvania State University, University Park, PA 16802, USA

<sup>j</sup> Alterra, Postbus 47, 6700 AA Wageningen, The Netherlands

<sup>k</sup> Department of Ecology and Environmental Research, Swedish University of Agricultural Sciences, S-750 07 Uppsala, Sweden

<sup>l</sup> INRA, Unité d'Ecophysiologie Forestière, F-54280 Champenoux, France

<sup>m</sup> Department of Environmental Research, Agricultural Research Institute, Keldnaholli, IS-112 Reykjavik, Iceland

<sup>n</sup> USDA Forest Service, 271 Mast Road, Durham, NH 03824, USA

<sup>o</sup> Research Group of Plant and Vegetation Ecology, Department of Biology, University of Antwerpen, Universiteitsplein 1, B-2610 Wilrijk, Antwerp, Belgium

<sup>p</sup> School of the Environment, Duke University, Box 90328, Durham, NC 27708-0328, USA

<sup>q</sup> Richardson Hall, Oregon State University, Corvallis, OR 97331-2209, USA

<sup>r</sup> NOAA/ATDD, 456 S. Illinois Avenue, Oak Ridge, TN 37831-2456, USA

<sup>s</sup> Department of Environmental, Population, and Organismic Biology, University of Colorado, Campus Box 334, Boulder, CO 80309, USA

<sup>t</sup> Department of Earth and Planetary Sciences, Harvard University, 20 Oxford St., Cambridge, MA 02138, USA

<sup>u</sup> Department of Biology, San Diego State University, San Diego, CA, USA

<sup>v</sup> Atmospheric Science Group, LAWR, UC Davis, 122 Hoagland Hall, Davis, CA 95616, USA

<sup>w</sup> Plant Biology and Biogeochemistry Department, Risoe National Laboratory, P.O. Box 49, DK-4000 Roskilde, Denmark

<sup>x</sup> Department of Physics, University of Helsinki, P.O. Box 9, FIN-00014 Helsinki, Finland

<sup>y</sup> Max-Planck-Institut für Biogeochemie, Tatzendpromenade 1a, 07701 Jena, Germany

<sup>z</sup> Department of Forest Environment and Resources, University of Tuscia, I-01100 Viterbo, Italy

\* Corresponding author. Tel.: +49-921-55-2576; fax: +49-921-55-2564.  
E-mail address: falge@uni-bayreuth.de (E. Falge).

40 **Abstract**

41 Differences in the seasonal pattern of assimilatory and respiratory processes are responsible for divergences in seasonal  
 42 net carbon exchange among ecosystems. Using FLUXNET data (<http://www.eosdis.ornl.gov/FLUXNET>) we have analyzed  
 43 seasonal patterns of gross primary productivity ( $F_{GPP}$ ), and ecosystem respiration ( $F_{RE}$ ) of boreal and temperate, deciduous  
 44 and coniferous forests, Mediterranean evergreen systems, a rainforest, temperate grasslands, and  $C_3$  and  $C_4$  crops. Based  
 45 on generalized seasonal patterns classifications of ecosystems into vegetation functional types can be evaluated for use in  
 46 global productivity and climate change models. The results of this study contribute to our understanding of respiratory costs  
 47 of assimilated carbon in various ecosystems.

48 Seasonal variability of  $F_{GPP}$  and  $F_{RE}$  of the investigated sites increased in the order tropical < Mediterranean <  
 49 temperate coniferous < temperate deciduous < boreal forests. Together with the boreal forest sites, the managed grass-  
 50 lands and crops show the largest seasonal variability. In the temperate coniferous forests, seasonal patterns of  $F_{GPP}$  and  $F_{RE}$   
 51 are in phase, in the temperate deciduous and boreal coniferous forests  $F_{RE}$  was delayed compared to  $F_{GPP}$ , resulting in the  
 52 greatest imbalance between respiratory and assimilatory fluxes early in the growing season.

53  $F_{GPP}$  adjusted for the length of the carbon uptake period decreased at the sampling sites across functional types in the  
 54 order  $C_4$  crops, temperate and boreal deciduous forests ( $7.5\text{--}8.3\text{ g C m}^{-2}$  per day) > temperate conifers,  $C_3$  grassland and  
 55 crops ( $5.7\text{--}6.9\text{ g C m}^{-2}$  per day) > boreal conifers ( $4.6\text{ g C m}^{-2}$  per day). Annual  $F_{GPP}$  and net ecosystem productivity ( $F_{NEP}$ )  
 56 decreased across climate zones in the order tropical > temperate > boreal. However, the decrease in  $F_{NEP}$  with latitude was  
 57 greater than the decrease in  $F_{GPP}$ , indicating a larger contribution of respiratory (especially heterotrophic) processes in boreal  
 58 systems.

59 © 2002 Published by Elsevier Science B.V.

60 *Keywords:* Season length; Gross primary production; Ecosystem respiration; FLUXNET; EUROFLUX; AmeriFlux; eddy covariance

61

62 **1. Introduction**

63 Ecosystem  $CO_2$  exchange is comprised of fluxes asso-  
 64 ciated with assimilatory and respiratory processes.  
 65 Timing and amplitude of these components determine  
 66 the seasonal pattern of net  $CO_2$  flux (Randerson et al.,  
 67 1999; White et al., 1999; Cramer et al., 1999). While at  
 68 temperate and high latitudes the period for assimilation  
 69 is usually restricted by temperature and moisture, res-  
 70 piratory processes continue throughout the year. Major  
 71 factors affecting the seasonal course and amount of  
 72 ecosystem gross primary production ( $F_{GPP}$ ), are sea-  
 73 sonal differences in leaf-area index, physiological ca-  
 74 pacity, meteorological conditions, and the length of  
 75 the growing season. Ecosystem respiration ( $F_{RE}$ ) as  
 76 the sum of heterotrophic respiration ( $F_{RH}$ ), and au-  
 77 totrophic respiration ( $F_{RA}$ ), is typically dominated by  
 78 disparate factors. The activity of soil microbes con-  
 79 tributes to  $F_{RH}$ , and is strongly regulated by soil tem-  
 80 perature and moisture status (Edwards, 1975; Lloyd  
 81 and Taylor, 1994; Davidson et al., 1998; Xu and Qi, in  
 82 press). While  $F_{RA}$  may be maintained over the course  
 83 of the year, the partitioning of autotrophic respiration  
 84 varies seasonally as the relative roles of growth and  
 85 maintenance respiration change. Periods of microbial

activity does not necessarily coincide with those where  
 green plants are photosynthetically active, as micro-  
 bial activity depends on suitable meteorological con-  
 ditions as well as on substrate availability and quality.  
 Clearly, it is the interplay between photosynthetic and  
 microbial active seasons, that determines the seasonal  
 pattern, phasing and amplitude of ecosystem energy  
 and material fluxes.

The balance between respiratory and assimilatory  
 processes is likely to be affected as a result of climate  
 change (Houghton et al., 1996). Systematic changes in  
 the length of the growing season (Keeling et al., 1996a;  
 Myneni et al., 1997; Hasenauer et al., 1999; Menzel  
 and Fabian, 1999; Randerson et al., 1999; Keyser et al.,  
 2000; Baldocchi et al., 2001) indicate an extension of  
 the period favorable for assimilation. The influence  
 of climate on respiratory processes is generally more  
 complicated. Soil respiration, for example, is strongly  
 coupled to soil temperature (Raich and Schlesinger,  
 1992; Lloyd and Taylor, 1994), however, in some  
 ecosystems microbial activity is affected by soil mois-  
 ture (e.g., Hanson et al., 1993; Fliebach et al., 1994;  
 Law et al., 2000). Soil models typically predict an ex-  
 ponential increase of soil respiration with temperature,  
 but with a secondary limitation by the quantity and

86  
87  
88  
89  
90  
91  
92  
93  
94  
95  
96  
97  
98  
99  
100  
101  
102  
103  
104  
105  
106  
107  
108  
109  
110

111 quality of the substrate for microbial activity (Rastetter  
112 et al., 1992). The feedbacks between temperature,  
113 moisture availability, and substrate properties seem to  
114 control the overall rate of soil respiration (Raich and  
115 Tufekciogul, 2000). In addition, temperature increases  
116 due to climate change are not evenly distributed over  
117 the time of the day with greater increases observed dur-  
118 ing night than in the day-time (Easterling et al., 1997).  
119 Shifts in the relative contribution of assimilation and  
120 respiration to total fluxes could affect future ecosystem  
121 carbon sequestration potentials, and the stability of  
122 stored carbon (Alward et al., 1999). On the other hand,  
123 potential shifts in photosynthetic and microbial activ-  
124 ities could reduce or reverse the benefits of increased  
125 growing season length to carbon sequestration.

126 At temperate and high latitudes carbon balances  
127 of terrestrial ecosystems undergo strong seasonal  
128 fluctuations. Growing season length strongly af-  
129 fects annual net ecosystem productivity ( $F_{NEP}$ )  $F_{NEP}$   
130 ( $=F_{GPP} - F_{RE}$ ), (Black et al., 1996, 2000; Goulden  
131 et al., 1998; Baldocchi et al., 2001; Meyers, in press),  
132 and ecosystem net primary production, ( $F_{NPP}$ )  $F_{NPP}$   
133 ( $=F_{GPP} - F_{RA}$ ) (Schulze et al., 1999). Model analy-  
134 ses suggest major impacts of growing season length  
135 on  $F_{NPP}$  (Field et al., 1998; White et al., 1999;  
136 Jackson et al., 2000). Average  $F_{NPP}$ , for example,  
137 varies among biomes between 0 and  $1.2 \text{ kg C m}^{-2}$  per  
138 year (Bergen and Dobson, 1999; Cramer et al., 1999;  
139 Goetz et al., 1999; Jiang et al., 1999; Nemry et al.,  
140 1999), but differences in  $F_{NPP}$  are much smaller  
141 when adjusted for the length of the growing season.  
142 These studies address seasonal fluctuations of the  
143 net fluxes,  $F_{NEP}$ , or  $F_{NPP}$ , but the component fluxes,  
144  $F_{GPP}$  and  $F_{RE}$ , often have dissimilar periods of activ-  
145 ity. For instance,  $F_{GPP}$  is strongly dependent on light  
146 during the growing season when temperature is ade-  
147 quate for growth, whereas  $F_{RE}$  is strongly dependent  
148 on temperature and moisture. Over the season light,  
149 temperature and moisture are out of phase, and this  
150 differs with latitude. Hence these drivers will affect  
151 net ecosystem carbon exchange ( $F_{NEE}$ ) differently  
152 as they force  $F_{GPP}$  and  $F_{RE}$  differently (Randerson  
153 et al., 1999). Consequently, we need to understand  
154 primarily the factors that influence the seasonality of  
155 the component fluxes,  $F_{RE}$  and  $F_{GPP}$ , and govern the  
156 seasonal patterns of net fluxes.

157 Tower-based observing systems based on microm-  
158 eteorological techniques provide means to directly

159 measure ( $F_{NEE}$ ), which differs from  $F_{NEP}$  by the  
160 amount of carbon exported from the system via  
161 run-off or harvest. Valentini et al. (2000) used data  
162 from a network of tower observations to obtain  $F_{RE}$   
163 and  $F_{GPP}$  by an extrapolation of site-specific expo-  
164 nential relationships between nocturnal fluxes and  
165 soil temperature into the day to calculate continuous  
166 records of  $F_{RE}$ . This approach allows us to investigate  
167 seasonal phasing and amplitudes of ecosystem respi-  
168 ration and assimilation. We make use of FLUXNET  
169 (<http://www.eosdis.ornl.gov/FLUXNET>), a data base  
170 with ecosystem  $\text{CO}_2$  flux ( $F_{NEE}$ ) and meteorologi-  
171 cal data obtained from tower-based systems between  
172 years 1992 and 2000. The sites on the European and  
173 American continents include deciduous and ever-  
174 green forests, grassland and crops, and cover a wide  
175 range of climatic zones, from boreal to tropical. The  
176 analysis provides valuable insight into the season-  
177 ality of respiration and assimilation for sites in a  
178 variety of ecotones, and better understanding of the  
179 processes that regulate  $F_{NEE}$ . This work contributes  
180 to our understanding of how well seasonal phas-  
181 ing and amplitudes of respiratory and assimilatory  
182 processes are currently represented in carbon cy-  
183 cle and soil–vegetation–atmosphere transfer (SVAT)  
184 models.

## 2. Methods

### 2.1. The data base and sites

187 FLUXNET (<http://www.eosdis.ornl.gov/FLUXN->  
188 [ET](http://www.eosdis.ornl.gov/FLUXNET)) hosts a data base of continuous measurements  
189 of ecosystem carbon and energy exchange, key me-  
190 teorological variables and ancillary data describing  
191 location, vegetation and climate of the sites. The  
192 data sets cover multiple years (1992–2000) of flux  
193 tower measurements from the AmeriFlux (23 sites)  
194 and EUROFLUX (16 sites, Valentini et al., 2000)  
195 projects. From these we selected 35 sites (Table 1),  
196 where night-time turbulence and hence  $F_{RE}$  could  
197 be assessed (details below). Mass and energy fluxes  
198 are measured with the eddy covariance technique  
199 (for details see, e.g., Aubinet et al. (2000)). The data  
200 undergo quality assurance, and missing half-hourly  
201 averages are filled using standardized methods to pro-  
202 vide complete data sets (Falge et al., 2001).

Table 1  
Vegetation type classification of 35 sites from the EUROFLUX and AmeriFlux projects<sup>a</sup>

Functional vegetation type	Site	Abbreviation	State/country
Temperate coniferous forests	Aberfeldy <sup>b</sup>	AB	UK
	WeidenBrunnen <sup>b</sup>	WE	Germany
	Tharandt <sup>b</sup>	TH	Germany
	Loobos <sup>b</sup>	LO	The Netherlands
	Brasschaat <sup>b</sup>	BR	Belgium
	Wind River <sup>c</sup>	WR	WA/USA
	Howland <sup>c</sup>	HL	ME/USA
	Metolius <sup>c</sup>	ME	OR/USA
	Duke Forest <sup>c</sup>	DU	NC/USA
High altitude coniferous forests	Niwot Ridge <sup>c</sup>	NR	CO/USA
Boreal coniferous forests	North Boreas <sup>c</sup>	NB	Man./Canada
	Flakaliden <sup>b</sup>	FL	Sweden
	Norunda <sup>b</sup>	NO	Sweden
	Hyytiala <sup>b</sup>	HY	Finland
Temperate deciduous forests	Vielsalm <sup>b</sup>	VI	Belgium
	Soroe <sup>b</sup>	SO	Denmark
	Hesse <sup>b</sup>	HE	France
	Harvard <sup>c</sup>	HV	MA/USA
	WalkerBranch <sup>c</sup>	WB	TN/USA
Cold temperate deciduous forests	Park Falls/WLEF	WL	WI/USA
	Willow Creek <sup>c</sup>	WC	WI/USA
Boreal deciduous forests	Gunnarsholt <sup>b</sup>	GU	Iceland
Maritime/Mediterranean evergreen forests	Bordeaux <sup>b</sup>	BO	France
	Castelporziano <sup>b</sup>	CP	Italy
	Sky Oaks young <sup>c</sup>	Skyoung	CA/USA
	Sky Oaks old <sup>c</sup>	Skold	CA/USA
	Blodgett Forest <sup>c</sup>	BL	CA/USA
Rainforest	Manaus <sup>c</sup>	MA	Brazil
Grasslands	LittleWashita <sup>c</sup>	LW	OK/USA
	Shidler <sup>c</sup>	SH	OK/USA
	Risoe <sup>b</sup>	RI	Denmark
Crops	Bondville <sup>c</sup>	Bvcorn	IL/USA
	Bondville <sup>c</sup>	Bvsoybean	IL/USA
	Ponca <sup>c</sup>	PO	OK/USA
	Soroe <sup>b</sup>	Sowheat	Denmark

<sup>a</sup> For more information on these sites see Falge et al. (2002).

<sup>b</sup> EUROFLUX projects.

<sup>c</sup> AmeriFlux projects.

## 203 2.2. The algorithms

### 204 2.2.1. Estimates of $F_{RE}$ and $F_{GPP}$

205 Ecosystem respiration,  $F_{RE}$ , is measured directly at  
 206 the towers during night-time periods with strong tur-  
 207 bulence (typically indicated by high surface momen-  
 208 tum flux, e.g., Goulden et al. (1996)), and was extrap-

olated to other periods by using exponential regres- 209  
 sions of measured  $F_{RE}$  with soil temperature. Alter- 210  
 native methods to estimate  $F_{RE}$  for periods when it 211  
 was not directly measured includes estimates from bio- 212  
 geochemical or SVAT models (e.g., Baldocchi et al., 213  
 2000), from chamber measurements extrapolated to 214  
 the stand scale (Law et al., 1999; Janssen et al., 2001; 215

216 Xu et al., 2001), or estimates derived from the regres-  
 217 sion of day-time  $F_{NEE}$  against photosynthetically ac-  
 218 tive radiation (PAR) (e.g., Suyker and Verma, 2001).  
 219 For the exponential regression here an Arrhenius equa-  
 220 tion (Eq. (1)) in the form reported by Lloyd and Taylor  
 221 (1994) was used.

$$222 F_{RE,night} = F_{RE,T_{ref}} e^{(E_a/R)((1/T_{ref})-(1/T_K))} \quad (1)$$

223 where  $F_{RE}$ ,  $T_{ref}$ , is the ecosystem respiration rate at  
 224  $T_{ref}$  (we used 283.16 K) and  $E_a$  the activation energy  
 225 in  $J mol^{-1}$  are fitted site-specific parameters,  $R$  the gas  
 226 constant ( $8.134 J K^{-1} mol^{-1}$ ), and  $T_K$  is the soil tem-  
 227 perature in a depth of 5 cm. The parameter  $F_{RE,T_{ref}}$   
 228 was evaluated for gliding 30-day period starting 1 Jan-  
 229 uary but  $E_a$  was kept constant over the entire year.  
 230 This might not be valid, as we expect changes in  $E_a$   
 231 due to changes in soil moisture conditions and the ef-  
 232 fects of growth and maintenance respiration. Yet, the  
 233 overall scatter typically found in the relationship be-  
 234 tween night-time  $T_K$  and  $F_{RE}$  determined by eddy co-  
 235 variance (e.g., Goulden et al., 1996) prevented us from  
 236 analyzing such effects. For more details on the qual-  
 237 ity of the fits see Appendix A (see Table 4). The de-  
 238 rived parameter sets were applied over the entire year  
 239 to obtain a continuous record of half-hourly data. Val-  
 240 ues of  $F_{GPP}$  were calculated as the difference between  
 241  $F_{RE}$  and  $F_{NEE}$ . For daily values of  $F_{RE}$  and  $F_{GPP}$  the  
 242 half-hourly results were summed. To address errors in  
 243 our  $F_{RE}$  (and subsequently  $F_{GPP}$ ) estimates, we com-  
 244 pared the estimates to values derived from light re-  
 245 sponses (hyperbolic relationship between  $F_{NEE}$  and  
 246 light, using Eq. (1) of Suyker and Verma (2001)).

#### 247 2.2.2. Maximum diurnal ecosystem respiration and 248 gross primary production

249 We used diurnal maximum fluxes,  $F_{RE}$  and  $F_{GPP}$ , to  
 250 assess the seasonal changes in rates of ecosystem res-  
 251 piration and assimilation. We calculated mean diurnal  
 252 cycles by bin-averaging the 30 min tower flux data for  
 253 intervals of 15 days (see Falge et al. (2002), Eq. (1)).  
 254 This time interval was chosen because a variety of  
 255 ecosystems fluxes show a spectral gap at this period  
 256 (Baldocchi et al., 2001). Missing data were filled by  
 257 look-up table methods based on meteorological condi-  
 258 tions (temperature and radiation for  $F_{GPP}$ , tempera-  
 259 ture for  $F_{RE}$ , see Falge et al. (2001)). This type of gap  
 260 filling was shown to introduce no bias errors (Falge  
 261 et al., 2001). Bin-averaging reduced sampling errors

by  $1/\sqrt{15}$  (Moncrieff et al., 1996), and the procedure  
 262 resulted in 350 (=365 – 15) mean diurnal courses per  
 263 year. The maximum values of  $F_{RE}$  and  $F_{GPP}$  for each  
 264 diurnal course were determined. Estimating averages  
 265 for 30-day period using Eq. (1) reduces random errors  
 266 of one-point eddy covariance measurements by a  
 267 factor of  $1/\sqrt{30}$  or 0.183, resulting in uncertainties of  
 268  $\pm 3\%$  for the mean of a 30-day period if the random  
 269 error is assumed to be 15%. This does not take into  
 270 account systematic errors potentially observed with  
 271 eddy covariance at night or on unfavorable terrain.  
 272 For a more detailed review of uncertainty estimates,  
 273 see Goulden et al. (1996) or Moncrieff et al. (1996).  
 274

### 275 3. Results

As  $F_{GPP}$  is calculated from the sum of  $F_{RE}$  and  
 276  $F_{NEP}$ , errors in  $F_{RE}$  affect the magnitude of  $F_{GPP}$  esti-  
 277 mates. Therefore we compared our estimates of  $F_{RE}$  to  
 278 values derived from the light response of  $F_{NEP}$  during  
 279 the growing season (April to mid September), where a  
 280 typical hyperbolic relationship between  $F_{NEP}$  and light  
 281 can be observed. The methods compare well for most  
 282 sites (Fig. 1): a linear regression yields a slope of 0.94  
 283 and an intercept of  $0.25 g C m^{-2}$  per day. Excluding  
 284 fluxes taken at night when evaluating light responses  
 285 of  $F_{NEP}$ , the above linear comparison has a similar  
 286 slope of 1.00 and intercept of  $-0.17 g C m^{-2}$  per day  
 287 but more scatter (data not shown). Three boreal sites  
 288 (Norunda, North Boreas, Gunnarsholt), and two crop  
 289 sites (Bondville, Soroe-Wheat) were not included in  
 290 the linear regression. We also excluded the prairie site  
 291 (Shidler), which yielded a 20% smaller estimate when  
 292  $F_{RE}$  is derived from light responses, a similar result as  
 293 reported in Suyker and Verma (2001). In particular, it  
 294 seems the methods do not compare well in boreal and  
 295 grass or crop ecosystems. This could be due to low  
 296 leaf-area indices with dead material and/or bare soil  
 297 intercepting photons in those systems, reducing pho-  
 298 tosynthetic light use efficiency. Also, these systems  
 299 (particularly Norunda) are losing lots of carbon from  
 300 below ground and other carbon pools, and deviations  
 301 in the estimates of  $F_{RE}$  eventually reveal the relative  
 302 differences between short term autotrophic carbon loss  
 303 versus longer term heterotrophic carbon loss.  
 304

Seasonal pattern of maximum and mean diurnal  
 305  $F_{GPP}$  and  $F_{RE}$  are shown for four sites in Fig. 2. As  
 306

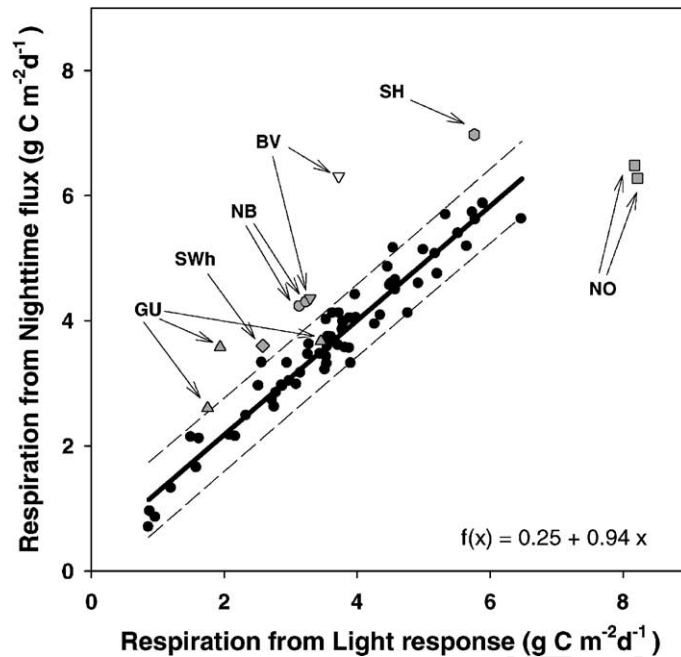


Fig. 1. Ecosystem respiration ( $F_{RE}$ ), calculated from light response relationships (Eq. (1) in Suyker and Verma, (2001)) compared to the values derived from exponential regressions between soil temperature and night-time fluxes under turbulent conditions (Eq. (1)). Data represent average daily sums for all days of the growing season where both methods could be applied. Three boreal sites (NO: Norunda; NB: North Boreas; GU: Gunnarsholt), two crop sites (BV: Bondville; SWh: Soroe-Wheat) and the prairie site (SH: Shidler) are not included in the linear regression.

307 simulation is active year-round in the temperate coniferous and the evergreen broad-leaf forest, and shows a very confined season in the deciduous and the boreal forest. With the exemption of the boreal coniferous forest—we find correspondence between the amount of assimilation and respiration, high respiration at high assimilation and low respiration at low assimilation rates. The seasonal course of mean  $F_{GPP}$  shows similar patterns, however the differences between mean  $F_{GPP}$  and  $F_{RE}$  are smaller than for diurnal maximum fluxes. Mean  $F_{GPP}$  and  $F_{RE}$  are mostly out of phase for the boreal conifers, but the temperate and Mediterranean systems show again the compensatory behavior of  $F_{GPP}$  and  $F_{RE}$ .

321 Fig. 3 shows maximum  $F_{GPP}$  for the temperate and boreal deciduous and coniferous forests.  $F_{GPP}$  could not be calculated for all sites due to incomplete data seasonal  $F_{RE}$ . Site specific data were smoothed by applying a 10-day moving average, and normalized to the maximum observed value during the year. Absolute maximum and minimum values and the corresponding day of the year are given in Table 2. We averaged the data for each site for all available years to reduce the sensitivity of the results to occasional large gaps in the data and to depict biome specific patterns rather than inter-annual variability. Seasonal courses of maximum  $F_{GPP}$  of the temperate and boreal forest sites show the pattern we found for net uptake (see Falge et al. (2002)), temperate conifers with the longest, boreal deciduous with the shortest, and temperate deciduous and boreal coniferous forests with intermediate and indeed very similar assimilation periods. The temperate coniferous forests and Vielsalm (VI), a mixed forest, show assimilation potential even in winter. The low assimilation rates at Brasschaat (BR) in April and May are probably due to anthropogenic influences ( $CO_2$  sources from residential areas). The assimilation potential of the high altitude coniferous forest site (Niwot Ridge, NW) is similar to the temperate deciduous forest sites, clearly point-

327  
328  
329  
330  
331  
332  
333  
334  
335  
336  
337  
338  
339  
340  
341  
342  
343  
344  
345  
346

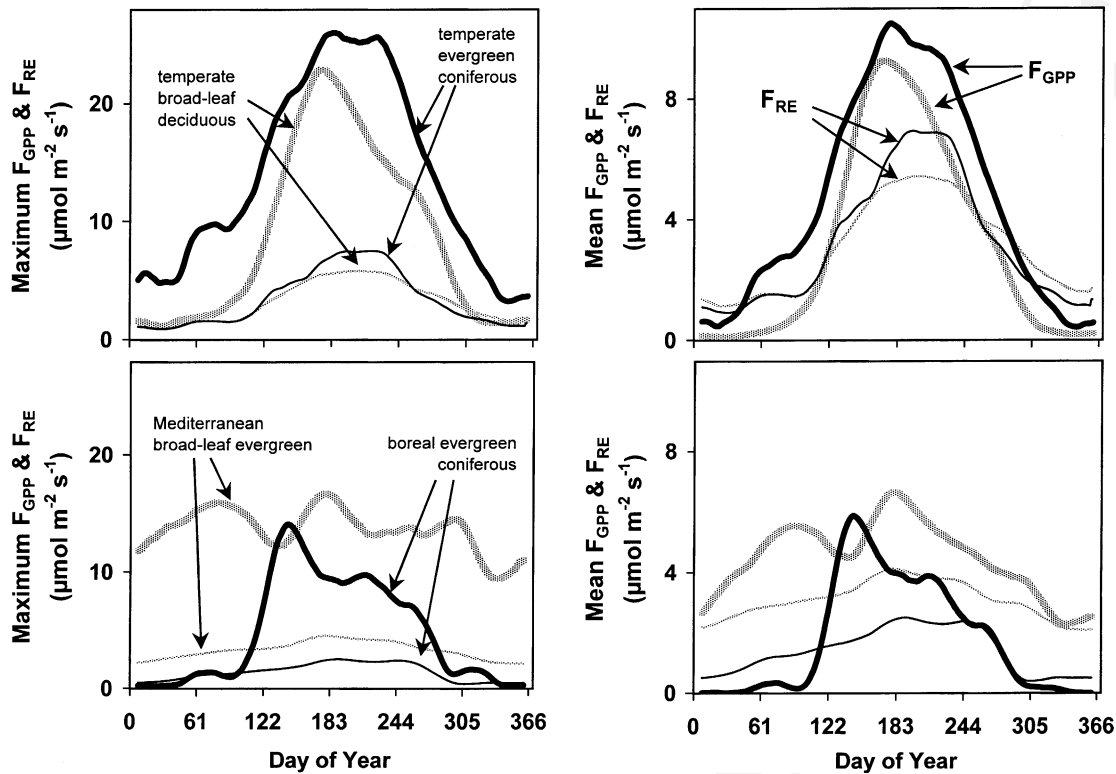


Fig. 2. Seasonal development of maximum mean diurnal ecosystem gross primary production ( $F_{GPP}$ ), and maximum diurnal ecosystem respiration ( $F_{RE}$ ), from 15-day bin-averaged data. Temperate forest sites are in the upper panel (Tharandt and Soroe), and Mediterranean and boreal are in the lower panel (Castelporziano and Flakaliden).

347 ing to a delayed phenology for conifers at high eleva-  
348 tions.

349 The results for the seasonal trends of maximum  $F_{RE}$   
350 are shown in Fig. 4. In general, they resemble the pat-  
351 terns we described for maximum night-time carbon  
352 release in Falge et al. (2002). However, there seems to  
353 be a more gradual transition between the patterns of  
354 the temperate conifers, temperate deciduous, and the  
355 boreal conifers, as we analyze  $F_{RE}$  during the entire  
356 day, i.e., maximum values are likely to occur during  
357 day-time when temperatures are higher. In general, the  
358 seasonal pattern in  $F_{RE}$  reveals a large influence of cli-  
359 mate (temperate versus boreal), whereas the life-form  
360 (deciduous or coniferous) seems to be less relevant for  
361 the seasonality of respiratory processes.

362 Figs. 5 and 6 summarize seasonal patterns of  $F_{GPP}$   
363 and  $F_{RE}$  for the sites of the remaining functional types,  
364 grassland, crops, maritime/Mediterranean ecosys-

365 tems, and a rainforest. Maximum  $F_{GPP}$  of the ever-  
366 green maritime and Mediterranean forests reflects  
367 their year-round assimilatory activity (Fig. 5), and  
368 maximum  $F_{RE}$  never drops below 25% of the max-  
369 imum observed value during the season. However,  
370 drought periods are likely to affect  $F_{RE}$  during late  
371 spring (CP), or summer (BL, BO). For the temperate  
372 grassland sites the phasing of maximum  $F_{RE}$   
373 (Fig. 6) corresponds well with the patterns observed  
374 in temperate deciduous forests, however the ampli-  
375 tudes differ: maximum  $F_{RE}$  in the forests (Fig. 4)  
376 does not decline to almost 0 in winter, as it is found  
377 for the grasslands. Crop sites often develop a second  
378 maximum in  $F_{GPP}$  after the harvest due to inter-crops  
379 or weeds, and several maximums in  $F_{RE}$  evidently  
380 following management practices (Fig. 6).

381 Summarizing Figs. 3–6, the seasonal patterns ob-  
382 served in Falge et al. (2002) are reflected in the results

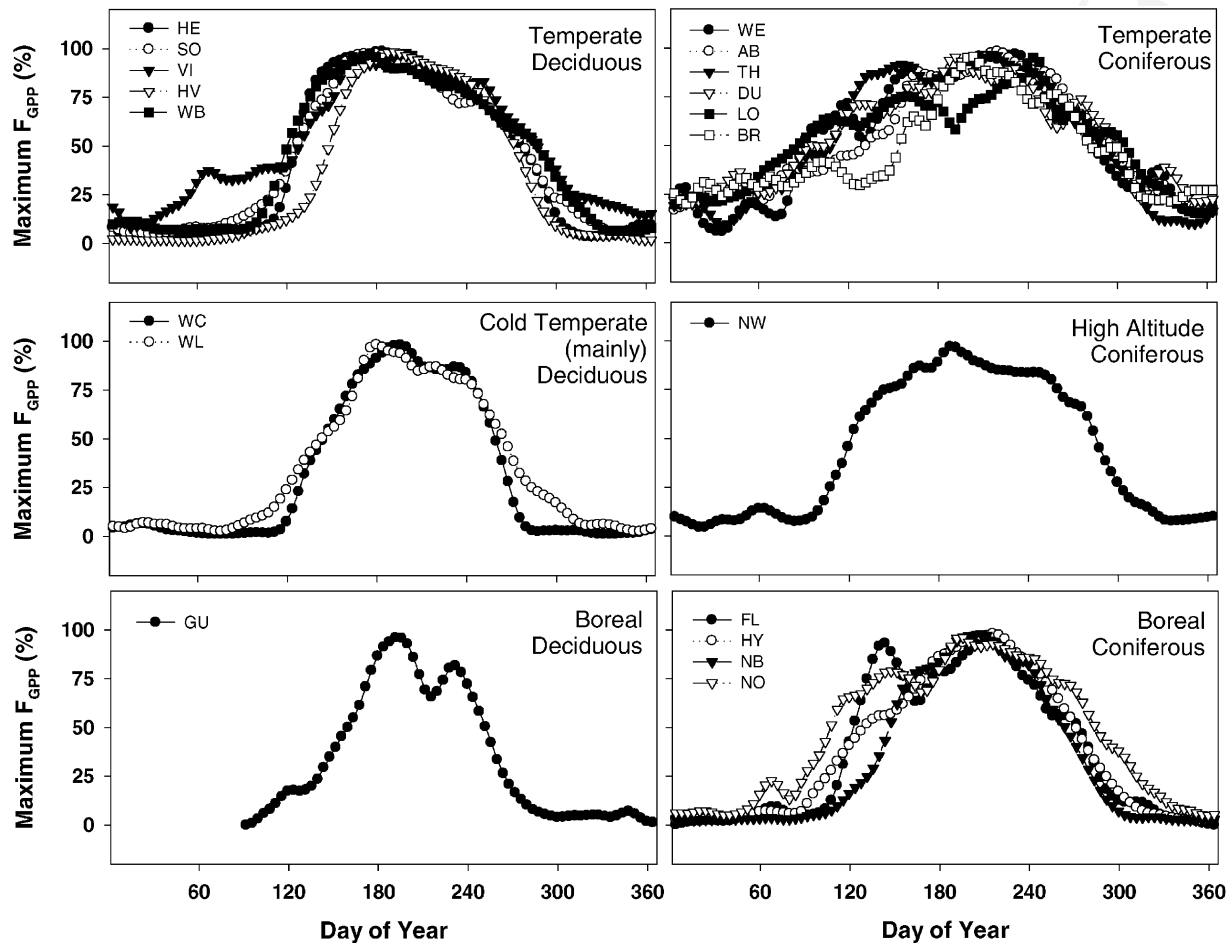


Fig. 3. Seasonal development of maximum diurnal  $F_{GPP}$ , for selected sites from Table 1, temperate, cold temperate, and boreal deciduous forests (left panels), and temperate, high altitude, and boreal coniferous forests (right panels). Data are normalized such that the maximum observed value equals 100%. Absolute maximum values are given in Table 2.

383 for  $F_{GPP}$  and  $F_{RE}$  and grouped for the sites in the  
 384 above functional types. Temperate deciduous and boreal  
 385 coniferous forest sites comprise one class in terms  
 386 of the seasonal phase and amplitude of  $F_{GPP}$ , whereas  
 387 temperate coniferous sites show a prolonged carbon  
 388 uptake period together with smaller amplitude. In contrast,  
 389 the seasonal course of  $F_{RE}$  of the temperate deciduous  
 390 forest sites matches the pattern found for the temperate  
 391 conifers, whereas the phasing of  $F_{RE}$  of boreal  
 392 conifers is shorter and the amplitude larger. Fig. 7  
 393 shows the difference between seasonal maximum (set  
 394 to 100%) and minimum  $F_{GPP}$  (values of sampling sites  
 395 averaged within vegetation functional types). Mini-

396 mum  $F_{GPP}$  amounts to 75% of the maximum in the  
 397 tropical system, 30% in the maritime/Mediterranean  
 398 evergreen systems, 12% in the temperate coniferous  
 399 systems, and 0–4% in the other systems as boreal  
 400 forest sites, temperate deciduous sites, grasslands  
 401 and crops. Similarly, minimum seasonal rates of  $F_{RE}$   
 402 amounts to 95% of maximum  $F_{RE}$  in the tropical,  
 403 35% in the maritime/Mediterranean, 14–17% in the  
 404 temperate forest sites (deciduous and coniferous),  
 405 9% in the boreal coniferous forests, and 4–6% in the  
 406 boreal deciduous forest, grassland and crop sites.

In Falge et al. (2001) we used the ratio between  
 407  $F_{GPP}$  and  $F_{RE}$  ( $z = F_{GPP}/F_{RE}$ ) to evaluate the relative  
 408



Table 2

Seasonal maximum and minimum of  $F_{GPP}$  and  $F_{RE}$ , together with the day of the year, where maximum and minimum rates occur, for 29 sites from the EUROFLUX and AmeriFlux projects<sup>a</sup>

Site	$F_{GPP}$		$F_{RE}$	
	Seasonal maximum ( $\mu\text{mol CO}_2 \text{ m}^{-2} \text{ s}^{-1}$ )	Seasonal minimum ( $\mu\text{mol CO}_2 \text{ m}^{-2} \text{ s}^{-1}$ )	Seasonal maximum ( $\mu\text{mol CO}_2 \text{ m}^{-2} \text{ s}^{-1}$ )	Seasonal minimum ( $\mu\text{mol CO}_2 \text{ m}^{-2} \text{ s}^{-1}$ )
Temperate coniferous forests				
Aberfeldy <sup>b</sup>	16.0 (216)	2.5 (1)	5.3 (225)	0.7 (3)
WeidenBrunnen <sup>b</sup>	18.3 (232)	0.7 (36)	7.3 (230)	1.4 (37)
Tharandt <sup>b</sup>	25.3 (216)	2.0 (34)	6.9 (215)	1.0 (35)
Loobos <sup>b</sup>	24.0 (246)	3.5 (351)	5.3 (177)	1.0 (7)
Brasschaat <sup>b</sup>	20.2 (202)	3.4 (12)	16 (172)	2.1 (72)
Duke Forest <sup>c</sup>	24.5 (191)	4.6 (8)	3.6 (206)	1.0 (65)
High altitude coniferous forests				
Niwot Ridge <sup>c</sup>	15.1 (186)	0.5 (23)	6.3 (185)	1.0 (353)
Boreal coniferous forests				
North Boreas <sup>c</sup>	18.1 (210)	0.4 (352)	12.8 (211)	0.3 (28)
Flakaliden <sup>b</sup>	13.2 (219)	0.0 (6)	4.1 (212)	0.5 (12)
Norunda <sup>b</sup>	30.4 (191)	1.4 (7)	8.6 (187)	1.2 (41)
Hyytiala <sup>b</sup>	13.1 (219)	0.2 (351)	4.0 (213)	0.3 (43)
Temperate deciduous forests				
Vielsalm <sup>b</sup>	21.5 (196)	1.6 (7)	21.5 (196)	1.6 (7)
Soroe <sup>b</sup>	25.3 (175)	1.1 (27)	6.8 (208)	1.2 (34)
Hesse <sup>b</sup>	24.8 (184)	0.6 (14)	7.4 (223)	0.8 (35)
Harvard <sup>c</sup>	25.0 (190)	0.4 (49)	4.7 (191)	1.0 (37)
Walker Branch <sup>c</sup>	29.9 (176)	1.8 (332)	3.9 (202)	0.4 (33)
Cold temperate deciduous forests				
Park Falls/WLEF <sup>c</sup>	19.6 (178)	0.4 (74)	7.9 (200)	0.3 (363)
Willow Creek <sup>c</sup>	28.3 (190)	0.2 (72)	5.7 (190)	0.5 (22)
Boreal deciduous forests				
Gunnarsholt <sup>b</sup>	23.0 (192)	0.2 (1)	13.6 (183)	0.1 (3)
Maritime/Mediterranean evergreen forests				
Bordeaux <sup>b</sup>	23.8 (159)	7.6 (339)	7.4 (177)	1.8 (29)
Castelporziano <sup>b</sup>	17.5 (178)	8.4 (338)	4.6 (172)	2.1 (4)
Blodgett Forest <sup>c</sup>	23.8 (159)	7.6 (339)	3.3 (343)	0.9 (257)
Rainforest				
Manaus <sup>c</sup>	29.5 (4)	22.3 (189)	7.2 (267)	6.9 (362)
Grasslands				
LittleWashita <sup>c</sup>	14.4 (176)	0.7 (356)	6.6 (181)	0.4 (362)
Shidler <sup>c</sup>	39.2 (182)	0.1 (24)	15.0 (176)	0.3 (14)
Crops				
Bondville <sup>c</sup> C4	60.5 (199)	0.3 (294)	15.8 (180)	0.1 (362)
Bondville <sup>c</sup> C3	27.3 (196)	0.3 (73)	8.7 (182)	0.0 (11)
Ponca <sup>c</sup>	33.5 (124)	1.7 (226)	6.0 (210)	1.4 (22)
Soroe <sup>b</sup>	31.7 (187)	0.2 (25)	10.8 (145)	0.0 (7)

<sup>a</sup> Data are averaged for all available years. Values of  $F_{GPP,max}$  and  $F_{RE,max}$  are derived as maximum values from a time series of  $F_{GPP}$  and  $F_{RE}$  using a 15-day running mean filter for each half-hour of the day. Values in parenthesis indicate the day of the year.

<sup>b</sup> EUROFLUX projects.

<sup>c</sup> AmeriFlux projects.

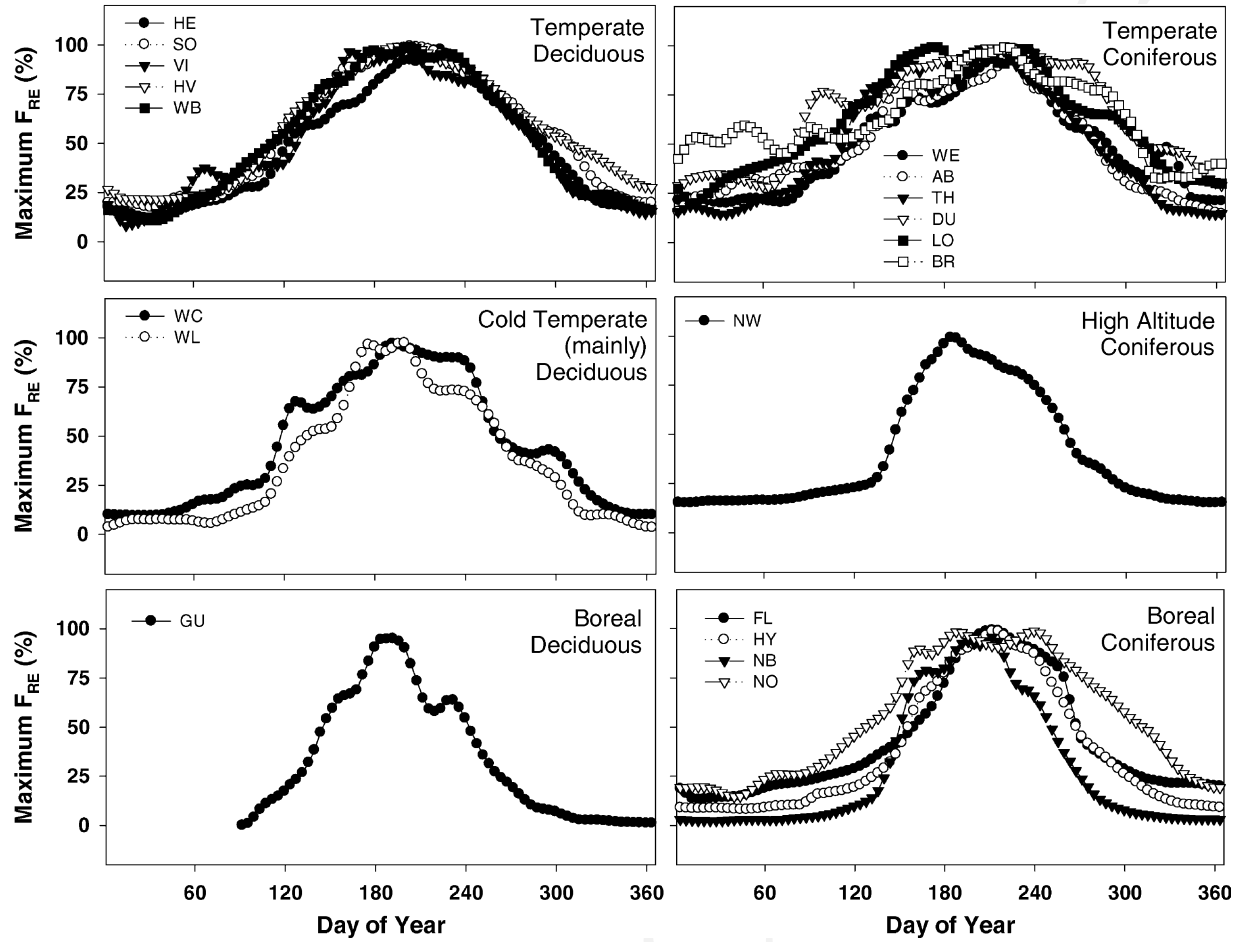


Fig. 4. As in Fig. 3, but for seasonal development of maximum diurnal  $F_{RE}$ , for selected sites from Table 1.

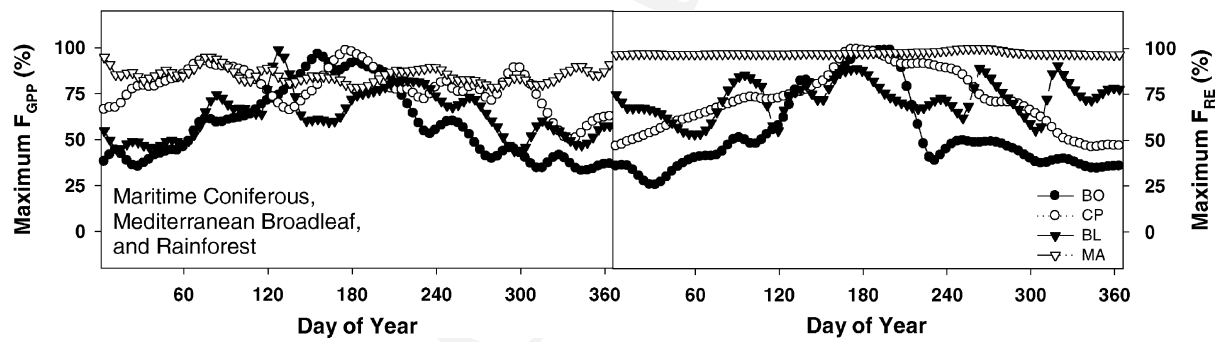


Fig. 5. Seasonal development of maximum diurnal  $F_{GPP}$  (left panel), and maximum mean diurnal  $F_{RE}$  (right panel), for maritime and Mediterranean evergreen forests from Table 1.

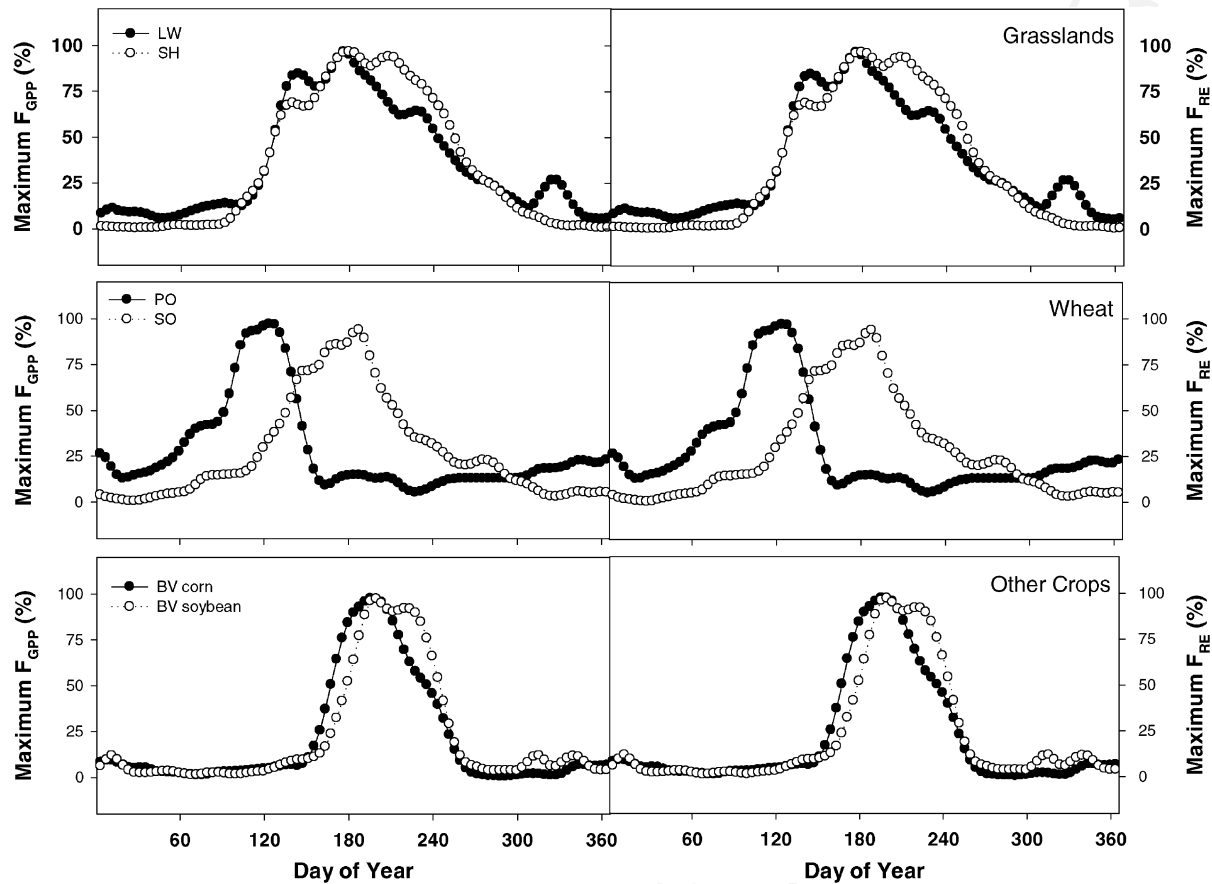


Fig. 6. Seasonal development of maximum diurnal  $F_{GPP}$  (left panel), and maximum diurnal  $F_{RE}$  (right panel), for grassland and crop ecosystems (Table 1).

409 contribution of carbon exchange processes to the total  
 410 annual exchange. This analysis illustrates what frac-  
 411 tion of assimilation is consumed by the plant or sup-  
 412 ports the activities of heterotrophs in the soil. Values  
 413 of  $z$  below 1 occur when the system becomes a source  
 414 of  $CO_2$ , while  $z = 1$  on an annual or decadal basis in-  
 415 dicates a system that is in carbon balance ( $F_{NEE} = 0$ ).  
 416 When  $F_{GPP}$  exceeds  $F_{RE}$  ( $z > 1$ ) the system is storing  
 417 carbon, usually observed in young “growing” stages.  
 418 When  $F_{GPP}$  substantially exceeds  $F_{RE}$  the system  
 419 has potential to deprive of free nutrients by accumu-  
 420 lating both carbon and available nutrients in (dead)  
 421 biomass. Considering the close link between soil  
 422 organic matter decomposition and nutrient cycling,  
 423 systems with low  $F_{RH}$  will likely show negative feed-  
 424 backs to growth and  $F_{GPP}$  or become susceptible to

disturbance (e.g., Schulze et al., 1999; Walker et al., 425  
 1999; Amiro, 2001). We calculated values of  $z$  from 426  
 monthly sums of  $F_{GPP}$  and  $F_{RE}$  over the course of 427  
 the year averaged for all available years for each site 428  
 (Fig. 8). The length of the period during which  $z$  429  
 was greater than 1 is a measure of the length of the 430  
 carbon uptake period (in days,  $S_{GPP/RE}$ , see Table 431  
 3). Carbon uptake periods were longest in the ever- 432  
 green systems such as Mediterranean and temperate 433  
 coniferous forests, shorter in the boreal and temperate 434  
 deciduous forests and native grasslands, and shortest 435  
 in the crop systems (not shown) and drought stressed 436  
 rangeland (LW). Values of  $z = 2$  (dotted lines in Fig. 437  
 8) correspond to  $F_{NEP} = F_{RE}$ , indicating low over- 438  
 all contribution of  $F_{RH}$ , suggesting that autotrophic 439  
 processes mainly govern ecosystem carbon fluxes, 440

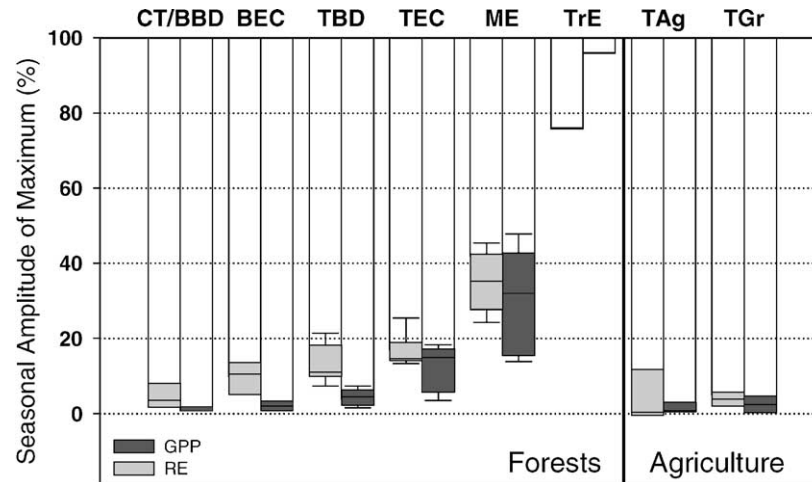


Fig. 7. Seasonal amplitudes of maximum ecosystem gross primary production,  $F_{GPP}$  and maximum ecosystem respiration,  $F_{RE}$ , grouped by functional type (CT/BBD: cold temperate broad-leaf deciduous; BEC: boreal evergreen conifers; TBD: temperate broad-leaf deciduous; TEC: temperate evergreen conifers; ME: maritime/Mediterranean evergreen forests; TrE: rainforest; TAg: temperate crops; TGr: temperate grasslands). Data are derived by calculating the ratio between minimum and maximum values reported in Table 2 in percentage, and averaged for each functional type. Box charts are used to emphasize total range, and median.

441 as was observed for the crops, the boreal coniferous  
 442 sites in spring and for some temperate deciduous and  
 443 coniferous forests over several months. In the bo-  
 444 real coniferous systems (Fig. 8a), the large  $z$ -values  
 445 in spring reflect physiological activity of the leaves  
 446 while heterotrophic processes are still slow due to low  
 447 soil temperatures (Goulden et al., 1998). Low values  
 448 of  $z$ , reflecting low rates of photosynthesis, are found  
 449 in drought stressed ecosystems (LW and BL, Fig. 8b).

#### 450 4. Discussion

451 In this study we presented phasing and ampli-  
 452 tude of ecosystem gross primary production ( $F_{GPP}$ ),  
 453 and ecosystem respiration ( $F_{RE}$ ) over the course of  
 454 the year. Data were obtained from eddy covariance  
 455 tower networks from sites of a variety of functional  
 456 vegetation types of the Northern Hemisphere, and a  
 457 tropical rainforest site. We derived seasonal patterns  
 458 of photosynthetic and respiratory activity, and investi-  
 459 gated ecosystem differences in the ratio of organic  
 460 carbon consumed ( $F_{RE}$ ) and produced ( $F_{GPP}$ ) within  
 461 the system.

462 Identification of functional types allows treating  
 463 groups of vegetation units or species as single entities

464 according to their specific interaction with the envi-  
 465 ronment. The usefulness of this concept depends on  
 466 the attributes selected for the classification. From a  
 467 functional perspective, ecosystems could be grouped  
 468 by their mass and energy exchange or productivity  
 469 and respiration rates. Applying a more morphologic  
 470 view, global models of climate change and produc-  
 471 tivity employ classification schemes by biome or  
 472 vegetation type, e.g., evergreen needle-leaf forest,  
 473 deciduous broad-leaf forest (Warnant et al., 1994;  
 474 Field et al., 1995; Sellers et al., 1996a,b; Kohlmaier  
 475 et al., 1997). We analyzed seasonal pattern of  $F_{GPP}$   
 476 and  $F_{RE}$  to test the potential to generalize functional  
 477 characteristics within currently applied classification  
 478 schemes.

479 Standard attributes in classification schemes of  
 480 global models are life-forms (e.g., deciduous or conif-  
 481 erous) and climate (e.g., temperate, boreal). Remark-  
 482 able parallels were found in seasonal pattern of net  
 483 ecosystem fluxes ( $F_{NEP}$ ) within and between groups  
 484 defined by life-form and climate zone (Falge et al.,  
 485 2002). In general, the seasonal patterns for  $F_{GPP}$  and  
 486  $F_{RE}$  from the sampling sites reflect the results ob-  
 487 served for  $F_{NEP}$ . The seasonal patterns of  $F_{RE}$  of the  
 488 temperate deciduous and coniferous forests are similar  
 489 in length to the active period, while the active season

490 for  $F_{RE}$  in the boreal conifers is shorter. In terms of  
 491  $F_{GPP}$ , in contrary, the temperate deciduous and boreal  
 492 coniferous forest sites are similar, whereas the temperate  
 493 conifers show a longer active season. The seasonal  
 494 amplitude of maximum rates of  $F_{GPP}$  and  $F_{RE}$  at the  
 495 investigated sites increases in the order tropical <  
 496 maritime/Mediterranean < temperate coniferous <  
 497 temperate deciduous < boreal evergreen forests <  
 498 cold temperate and boreal deciduous forests. Again,  
 499 the temperate and boreal coniferous forests fall in two  
 500 different classes. Thus, climate has a large impact on  
 501 the seasonal pattern in  $F_{RE}$  while life-form dictates  
 502 the seasonality of assimilatory processes.

503 We assessed ecosystem carbon balances by analyzing  
 504 the ratio between  $F_{GPP}$  and  $F_{RE}$  ( $z = F_{GPP}/F_{RE}$ ,  
 505 Falge et al., 2001). When  $z > 1$  on an annual or  
 506 decadal basis the system is storing carbon, when  $z =$   
 507 1 the system is in carbon balance, and  $F_{RH}$  equals  
 508  $F_{NPP}$ . Typically, the ratio  $F_{GPP}/F_{RE}$  was between 1  
 509 and 2 during the growing season and below 1 during  
 510 the dormant period, showing the use of stored carbon  
 511 during this phase. Sites with prolonged periods  
 512 of values of 2 ( $F_{NEP} = F_{RE}$ ) and higher could indicate  
 513 problems during application of the eddy covariance  
 514 method, as  $F_{GPP}/F_{RE}$  will likely be overestimated  
 when  $F_{RE}$  is underestimated (e.g., due to problems

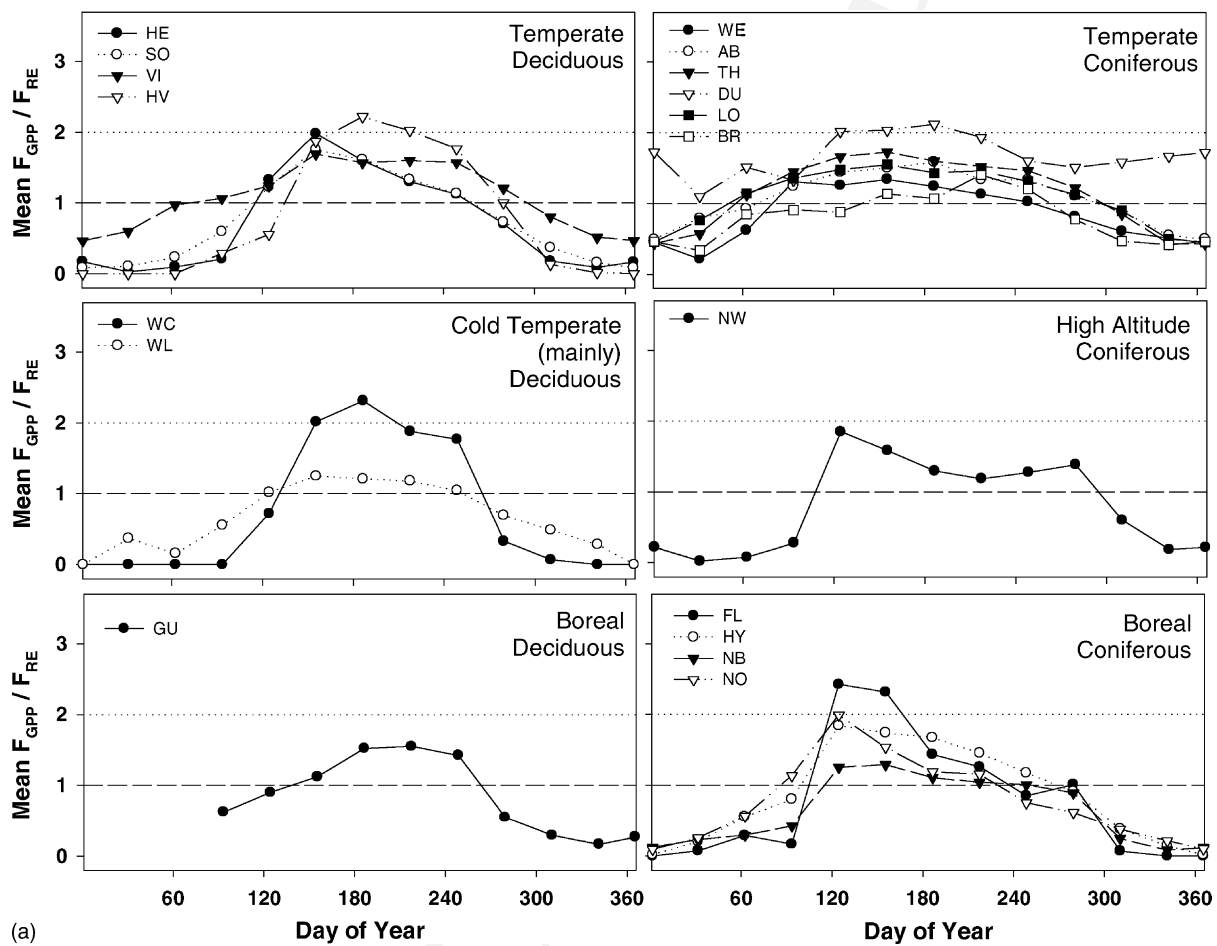


Fig. 8. Seasonal development of the ratio between  $F_{GPP}$  and  $F_{RE}$  for selected sites from Table 1. (a) Temperate, cold temperate, the boreal deciduous forests; (b) temperate, high altitude, and the boreal coniferous forests. The  $z$ -value of 1 (dashed lines) indicates that  $F_{NEP}$  equals 0. The  $z$ -value of 2 (dotted lines) corresponds to  $F_{NEP}$  equals  $F_{RE}$ , indicating low overall contribution of  $F_{RH}$ .

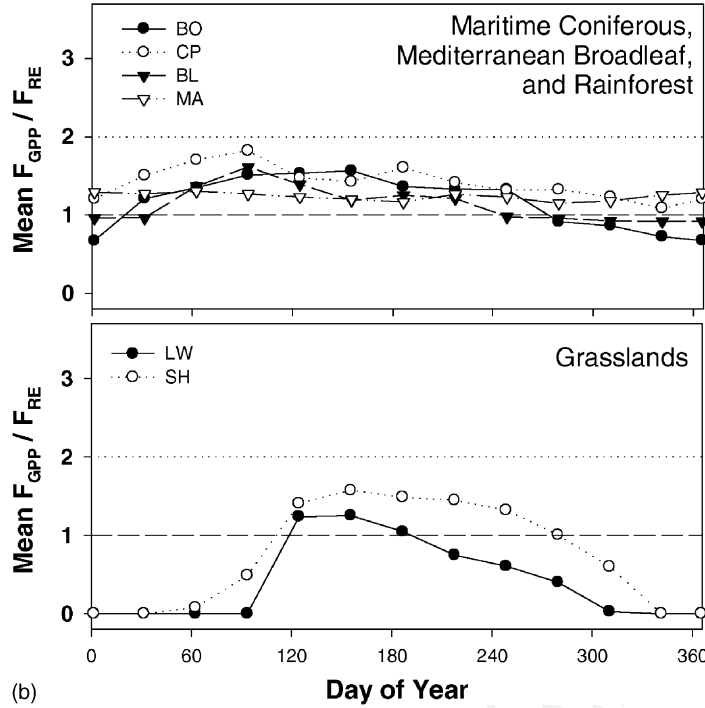


Fig. 8. (Continued).

Table 3

Annual sum of  $F_{GPP}$  and  $F_{NEP}$  estimates of the length of the carbon uptake period, and values of  $F_{GPP}$  and  $F_{NEP}$  adjusted for season length ( $F_{GPP}^d$  and  $F_{NEP}^d$ ) for 35 sites from the EUROFLUX and AmeriFlux projects<sup>a</sup>

Site	$F_{GPP}$ (g C m <sup>-2</sup> per year)	$F_{NEP}$ (g C m <sup>-2</sup> per year)	$S_{GPP/RE}$ (days)	$S_{NEP}$ (days)	$F_{GPP}^d$ (g C m <sup>-2</sup> per day)	$F_{NEP}^d$ (g C m <sup>-2</sup> per day)
Temperate coniferous forests						
Aberfeldy <sup>b</sup>	1924	597	289	307	6.27	1.95
WeidenBrunnen <sup>b</sup>	1319	-9	146	164	8.04	-0.06
Tharandt <sup>b</sup>	1806	628	257	266	6.79	2.36
Loobos <sup>b</sup>	1394	254	212	213	6.54	1.19
Brasschaat <sup>b</sup>	992	-146	136	173	5.74	-0.84
Wind River <sup>c</sup>	NA	327	NA	365	NA	0.90
Metolius <sup>c</sup>	1570	273	292	365	4.30	0.75
Duke Forest <sup>c</sup>	1487	595	318	339	4.39	1.75
High altitude coniferous forests						
Niwot Ridge <sup>c</sup>	831	71	180	189	4.40	0.38
Boreal coniferous forests						
North Boreas <sup>c</sup>	812	6	142	164	4.95	0.04
Flakaliden <sup>b</sup>	723	115	135	167	4.33	0.69
Norunda <sup>b</sup>	1691	-11	144	142	11.91	-0.08
Hyytiala <sup>b</sup>	959	246	173	182	5.27	1.35
Howland <sup>c</sup>	909	251	195	232	3.92	1.08

Table 3 (Continued)

Site	$F_{GPP}$ (g C m <sup>-2</sup> per year)	$F_{NEP}$ (g C m <sup>-2</sup> per year)	$S_{GPP/RE}$ (days)	$S_{NEP}$ (days)	$F_{GPP}^d$ (g C m <sup>-2</sup> per day)	$F_{NEP}^d$ (g C m <sup>-2</sup> per day)
Temperate deciduous forests						
Vielsalm <sup>b</sup>	1507	435	218	261	5.77	1.67
Soroe <sup>b</sup>	1276	91	139	141	9.05	0.64
Hesse <sup>b</sup>	1258	129	146	148	8.50	0.87
WalkerBranch <sup>c</sup>	1473	757	216	197	7.48	3.84
Harvard <sup>c</sup>	1122	181	142	138	8.13	1.31
Cold temperate deciduous forests						
Willow Creek <sup>c</sup>	1165	313	134	138	8.44	2.26
Park Falls/WLEF <sup>c</sup>	903	-22	109	136	6.64	-0.16
Boreal deciduous forests						
Gunnarsholt <sup>b</sup>	NA	NA	NA	108	NA	NA
Maritime/Mediterranean evergreen forests						
Bordeaux <sup>b</sup>	1681	454	255	300	5.60	1.51
Castelporziano <sup>b</sup>	1683	585	325	324	5.19	1.81
Sky Oaks young <sup>c</sup>	387	60	174	183	2.11	0.33
Sky Oaks old <sup>c</sup>	734	67	144	168	4.37	0.40
Blodgett Forest <sup>c</sup>	1386	339	256	272	5.10	1.24
Rainforest						
Manaus <sup>c</sup>	3249	608	365	365	8.90	1.66
Grasslands						
LittleWashita <sup>c</sup>	542	-212	65	86	6.30	-2.46
Shidler <sup>c</sup>	1715	362	154	160	10.72	2.26
Risoe <sup>b</sup>	NA	538	NA	253	NA	2.13
Crops						
Bondville <sup>c</sup> C4	1471	588	140	188	7.82	3.13
Bondville <sup>c</sup> C3	599	-115	85	90	6.66	-1.27
Ponca <sup>c</sup>	1396	155	176	211	6.62	0.74
Soroe <sup>b</sup>	1101	303	163	146	7.54	2.08

<sup>a</sup> EUROFLUX projects.

<sup>b</sup> The  $F_{NEP}$  based season length ( $S_{NEP}$ ) is number of days between spring and fall sign change of  $F_{NEP}$  (for crops uptake-period of inter-crops is included).  $S_{GPP/RE}$  is the length of the period, where  $z = F_{GPP}/F_{RE}$  was greater than 1. Values of  $F_{GPP}^d$  and  $F_{NEP}^d$  are calculated based on  $S_{NEP}$ . Data are averaged for all available years.

<sup>c</sup> AmeriFlux projects.

515 in nocturnal flux measurements, see below). Gener-  
516 ally, values of  $F_{GPP}/F_{RE}$  as derived from eddy co-  
517 variance measurements are high in comparison with  
518 model estimates of ecosystem metabolism, for exam-  
519 ple, seven of eight terrestrial biosphere models evalu-  
520 ated by Nemry et al. (1999) assume or calculate an-  
521 nual equilibrium between  $F_{RH}$  and  $F_{NPP}$  (or  $z = 1$ )  
522 for all locations. Values of  $z$  above 1 could be symp-  
523 tomatic for eddy covariance measurements, because of  
524 known uncertainties, especially concerning night-time  
525 fluxes or flux measurements in complex terrain (e.g.,  
526 Baldocchi et al., 2000; Aubinet et al., 2000). But they  
527 are supported by other evidence pointing to a large

528 northern hemispheric terrestrial carbon sink (e.g., Tans  
529 et al., 1990; Friedlingstein et al., 1995; Keeling et al.,  
530 1996b; Fan et al., 1998; Ciais et al., 1999).

531 In principle, an estimate of the photosynthetically  
532 active season could be derived from the numbers of  
533 days where  $F_{GPP}$  is larger than 0. However, the uncer-  
534 tainty of  $F_{RE}$  estimates is relatively large, eventually  
535 leading to positive  $F_{GPP}$  during dormant seasons, as  
536  $F_{GPP}$  is calculated as the sum of  $F_{NEP}$  and  $F_{RE}$ . There-  
537 fore the length of the season was determined by (1)  
538 calculating the time span between spring and fall sign  
539 change in  $F_{NEE}$ , and (2) by counting all days where  
540  $F_{GPP}/F_{RE} > 1$ , i.e.,  $F_{NEP}$  is positive (Table 3,  $S_{NEP}$

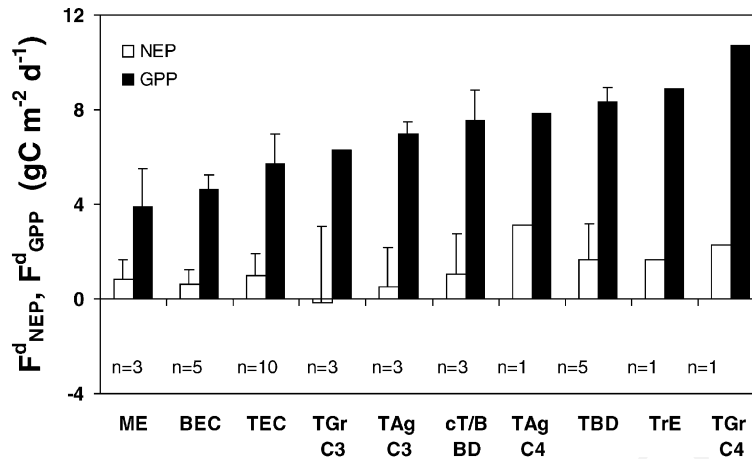


Fig. 9.  $F_{GPP}$  and  $F_{NEP}$  adjusted for length of the carbon uptake period, and averaged for functional vegetation types (ME: Mediterranean evergreen systems; BEC: boreal evergreen conifers; TrE: rainforest; TGr C3: temperate C<sub>3</sub> grasslands; TAg C3: temperate C<sub>3</sub> crops; TEC: temperate evergreen conifers; TAg C4: temperate C<sub>4</sub> crops; TBD: temperate broad-leaf deciduous; TGr C4: temperate C<sub>4</sub> grasslands. Vertical bars indicate standard deviation of the mean.

541 and  $S_{GPP/RE}$ , respectively). Annual sums of  $F_{GPP}$  and  
 542  $F_{NEP}$  were divided by  $S_{NEP}$  to determine  $F_{GPP}^d$  and  
 543  $F_{NEP}^d$ , values of  $F_{GPP}$  and  $F_{NEP}$  adjusted for the length  
 544 of the season. A comparison of these numbers averaged  
 545 for functional or biome type is given in Fig. 9.  
 546 Similar values were found for  $F_{GPP}^d$  at the C<sub>4</sub> crop  
 547 systems and temperate and cold temperate/boreal dec-  
 548 iduous forest sites (7.8, 8.3 and 7.5 g C m<sup>-2</sup> per day),  
 549 for the temperate conifers, C<sub>3</sub> crops and C<sub>3</sub> grass-  
 550 lands (5.7, 6.9 and 6.3 g C m<sup>-2</sup> per day, respectively),  
 551 and the boreal conifers (4.6 g C m<sup>-2</sup> per day). Values  
 552 for the Mediterranean systems and a C<sub>4</sub> grassland  
 553 were 3.9 and 10.7 g C m<sup>-2</sup> per day, the rate at the  
 554 tropical site was 8.9 g C m<sup>-2</sup> per day. The patterns  
 555 observed for  $F_{GPP}^d$  were not reproduced in patterns in  
 556  $F_{NEP}^d$  which decreased from 3.1 to -0.2 g C m<sup>-2</sup> per  
 557 day in the order C<sub>4</sub> crops > C<sub>4</sub> grasslands >  
 558 temperate deciduous forests, and rainforest >  
 559 cold temperate/boreal deciduous forests > temperate  
 560 conifers > Mediterranean systems > boreal conifers >  
 561 C<sub>3</sub> crops > C<sub>3</sub> grasslands. The results for the grass-  
 562 lands might be biased due severe drought in one C<sub>3</sub>  
 563 system, and the fact that the C-loss during prescribed  
 564 burning in the C<sub>4</sub> system is not included in the data.  
 565 In general,  $F_{NEP}^d$  is positive indicating nearly all of  
 566 the ecosystems in this study represent net sinks for at-  
 567 mospheric CO<sub>2</sub>. These tower-based estimates need to

568 be confirmed by other methods, for example based on  
 569 careful allometry. Nevertheless, the overall observed  
 570 patterns are reasonable, for instance the C<sub>4</sub> systems  
 571 showing higher carbon uptake than the C<sub>3</sub> systems,  
 572 or the relative consistency within the temperate C<sub>3</sub>  
 573 systems (with the exception of temperate deciduous  
 574 forest sites).

575 Eddy covariance data do not provide values of  $F_{NPP}$   
 576 (net primary productivity =  $F_{NEP} + F_{RH}$ ), and there  
 577 are no direct methods to estimate  $F_{NPP}$  from  $F_{NEP}$   
 578 or  $F_{GPP}$ . Separate measurements of  $F_{RH}$  would be  
 579 needed. However,  $F_{NPP}$  is the traditional measure of  
 580 plant productivity in forestry and agriculture and ex-  
 581 tensive data sets are available. More recently measure-  
 582 ments of  $F_{NPP}$  have been used to parameterize and  
 583 evaluate models of terrestrial carbon cycling to as-  
 584 sess the impacts of global land-use and climate change  
 585 (e.g., Cramer et al., 1999; Jiang et al., 1999; Nemry  
 586 et al., 1999), and for validation of remote sensing data  
 587 (Field et al., 1995; Goetz et al., 1999; Running et al.,  
 588 1999). We used three different sources of  $F_{NPP}$  data of  
 589 various vegetation types (Lieth, 1975; Schulze, 1982;  
 590 Waring and Schlesinger, 1985) for comparison with  
 591 annual  $F_{NEP}$  and  $F_{GPP}$  derived from eddy covariance  
 592 measurements (Fig. 10). A ratio of 0.45 was used to  
 593 convert biomass dry weight to carbon content, if ap-  
 594 plicable. For the forest ecosystems annual  $F_{GPP}$ ,  $F_{NPP}$



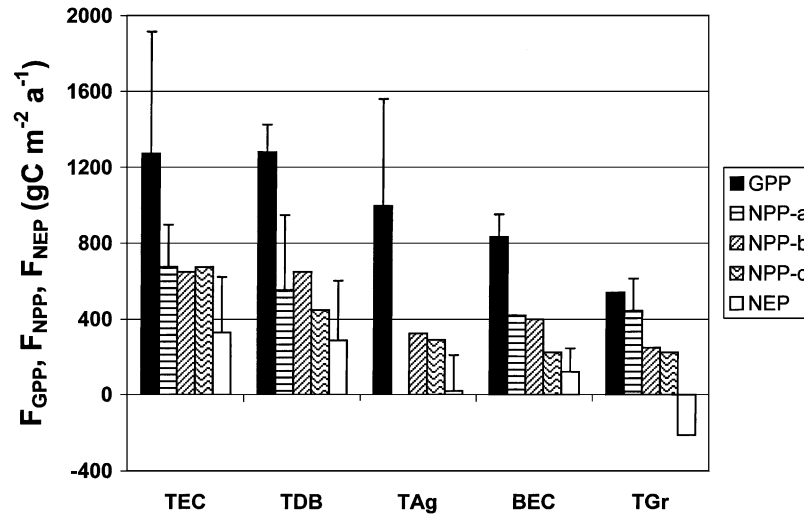


Fig. 10. Average  $F_{GPP}$ ,  $F_{NPP}$  and  $F_{NEP}$  for different vegetation types: TEC, temperate evergreen conifers; TDB, temperate deciduous broad-leaf forest; TAg, temperate crops; BEC, boreal evergreen conifers; TGr, temperate grasslands. Vertical bars indicate standard deviation of the mean.  $F_{GPP}$ , and  $F_{NEP}$  are derived from the eddy covariance data of this study. The three  $F_{NPP}$  estimates are from (a) Schulze (1982), (b) Waring and Schlesinger (1985), and (c) Lieth (1975).

595 and  $F_{NEP}$  all decreased comparing the temperate and  
 596 boreal zones. However, the decrease in  $F_{NEP}$  is greater  
 597 than in  $F_{NPP}$  or  $F_{GPP}$ . Our results show a strong lati-  
 598 tudinal trend in the ratio  $F_{NEP}/F_{GPP}$  for forest ecosys-  
 599 tems: 26% for the temperate evergreen conifers, 23%  
 600 for the temperate deciduous broad-leaf forests, and  
 601 15% for the boreal evergreen conifers. The relative  
 602 contribution of  $F_{NPP}$  to  $F_{GPP}$  is more constant: 51%  
 603 for the temperate evergreen conifers and temperate  
 604 deciduous broad-leaf forests, and 48% for the boreal  
 605 evergreen conifers. These values highlight a similar  
 606 contribution of autotrophic respiration to ecosystem  
 607 carbon metabolism in the temperate and the boreal  
 608 systems (49–52%). On the other hand, total respira-  
 609 tory costs of assimilated carbon are higher in the bo-  
 610 real systems (85% for boreal systems compared to  
 611 74–77% for temperate), indicating a larger contribu-  
 612 tion of  $F_{RH}$  to total ecosystem respiration in boreal  
 613 systems.

## 614 5. Conclusion

615 Using tower-base ecosystem-atmosphere exchange  
 616 data from the FLUXNET database, we have inves-

617 tigated seasonal patterns of  $F_{GPP}$ , and  $F_{RE}$ , derived  
 618 values of  $F_{NEE}$  and  $F_{GPP}$  adjusted for length of the  
 619 carbon uptake period and compared annual  $F_{GPP}$  with  
 620  $F_{NPP}$  from inventory studies for sites from a series of  
 621 functional vegetation types. The analysis included bo-  
 622 real and temperate, deciduous and coniferous forests,  
 623 Mediterranean evergreen systems, a rainforest, tem-  
 624 perate grasslands, and  $C_3$  and  $C_4$  crops.

625 Striking parallels in the seasonal pattern of  $F_{GPP}$   
 626 and  $F_{RE}$  were observed within and between the vege-  
 627 tation types, in terms of seasonal amplitude and phas-  
 628 ing of net carbon fluxes, and the relative contribution  
 629 of photosynthesis and respiration. Our results indicate  
 630 that temperate and boreal conifers should be viewed as  
 631 separate classes. Generalized seasonal patterns might  
 632 be utilized by global modelers and in inversion studies,  
 633 and to validate the phenology modules of plot scale  
 634 models.

635 For the temperate deciduous and boreal conifers, we  
 636 identified periods of unbalanced respiratory and assim-  
 637 ilatory processes, indicating a potentially higher sus-  
 638 ceptibility to changes in management practices or cli-  
 639 matic conditions, especially considering the expected  
 640 larger increase in night-time temperatures globally,  
 641 and greater temperature increases at high latitudes.

Table 4

Minimum, maximum, average and standard deviation of regression coefficients  $R^2$  of 32 sites from the EUROFLUX and AmeriFlux projects

Site	Year	$R^2$				Periods ( <i>n</i> )
		Minimum	Maximum	Average	S.D.	
Temperate coniferous forests						
Aberfeldy <sup>a</sup>	1998	0.793	0.97	0.902	0.049	335
WeidenBrunnen <sup>a</sup>	1998	0.539	0.969	0.871	0.105	317
Tharandt <sup>a</sup>	1999	0.336	0.864	0.696	0.164	335
Loobos <sup>a</sup>	1997	0.12	0.89	0.721	0.127	322
Brasschaat <sup>a</sup>	1998	0.22	0.845	0.683	0.14	321
Wind River <sup>b</sup>	1998	0.12	0.615	0.373	0.16	223
Howland <sup>b</sup>	1997	0.102	0.705	0.493	0.174	335
Duke Forest <sup>b</sup>	1999	0.288	1	0.604	0.162	305
High altitude coniferous forests						
Niwot Ridge <sup>b</sup>	2000	0.543	0.977	0.809	0.127	335
Boreal coniferous forests						
North Boreas <sup>b</sup>	1995	0.162	0.926	0.682	0.239	335
Flakaliden <sup>a</sup>	1997	0.16	0.86	0.717	0.138	330
Norunda <sup>a</sup>	1997	0.221	0.818	0.645	0.138	335
Hyytiala <sup>a</sup>	1998	0.206	0.975	0.751	0.248	335
Temperate deciduous forests						
Vielsalm <sup>a</sup>	1998	0.131	0.596	0.382	0.109	335
Soroe <sup>a</sup>	1997	0.246	0.952	0.686	0.216	335
Hesse <sup>a</sup>	1998	0.461	0.871	0.718	0.1	335
Harvard <sup>b</sup>	1999	0.441	0.902	0.774	0.092	335
WalkerBranch <sup>b</sup>	1998	0.123	0.67	0.445	0.157	335
Cold temperate deciduous forests						
Park Falls/WLEF	1998	0.173	0.873	0.587	0.182	335
Willow Creek <sup>b</sup>	2000	0.29	0.841	0.685	0.125	335
Boreal deciduous forests						
Gunnarsholt <sup>a</sup>	1997	0.277	0.978	0.805	0.173	263
Maritime/Mediterranean evergreen forests						
Bordeaux <sup>a</sup>	1998	0.885	0.992	0.947	0.03	181
Castelporziano <sup>a</sup>	1997	0.614	0.773	0.704	0.032	335
Sky Oaks young <sup>b</sup>	1998	0.607	0.999	0.832	0.092	207
Sky Oaks old <sup>b</sup>	1998	0.91	1	0.966	0.023	101
Blodgett Forest <sup>b</sup>	2000	0.642	0.999	0.85	0.066	152
Grasslands						
LittleWashita <sup>b</sup>	1998	0.053	0.897	0.6	0.224	289
Shidler <sup>b</sup>	1997	0.306	0.973	0.824	0.2	335
Crops						
Bondville <sup>b</sup>	2000	0.051	0.964	0.574	0.288	332
Bondville <sup>b</sup>	1997	0.057	0.874	0.49	0.291	305
Ponca <sup>b</sup>	1997	0.781	0.979	0.894	0.042	229
Soroe <sup>a</sup>	1999	0.101	0.761	0.466	0.147	280

<sup>a</sup> EUROFLUX projects.<sup>b</sup> AmeriFlux projects.

642 Overall, most of the sites we investigated sequester  
643 carbon, supporting the widely reported northern hemi-  
644 spheric terrestrial biosphere sink.

645 Our observation that  $F_{GPP}^d$ , adjusted for the length  
646 of the season, is not constant over various func-  
647 tional vegetation types and has important valida-  
648 tion potential for global carbon cycle modeling. For  
649 the sites in this study, values of  $F_{GPP}^d$  decreased  
650 from 10.7 to 2.4 g C m<sup>-2</sup> per day in the order C<sub>4</sub>  
651 grassland > rainforest > C<sub>4</sub> crops and temperate de-  
652 ciduous forests > C<sub>3</sub> crops, grassland and temperate  
653 conifers > boreal conifers > Mediterranean systems.

654 To investigate the impacts of global land-use and  
655 climate change, models of terrestrial carbon cycling  
656 and validation approaches of remote sensing data pri-  
657 marily assess  $F_{NPP}$ . Comparing  $F_{NPP}$  from various lit-  
658 erature sources with annual values of  $F_{NEP}$  and  $F_{GPP}$   
659 well-known latitudinal gradients were confirmed, and  
660 the relative contribution of  $F_{RH}$  to the total respiratory  
661 costs of assimilation of various vegetation types was  
662 estimated. However, our ability to compare our results  
663 directly to on-site estimates of  $F_{NPP}$  is constrained by  
664 the lack of sites where both long-term eddy covari-  
665 ance data and measurements of net primary produc-  
666 tivity are available. To overcome these limitations fu-  
667 ture investigations at tower sites should preferably be  
668 complemented by inventory studies of carbon stock  
669 changes.

## 670 Uncited references

671 [Lee \(1998\)](#) and [Valentini \(2000\)](#).

## 672 Acknowledgements

673 This work is supported by the BMBF project  
674 BITÖK (PT BEO 51-0339476) and the FLUXNET  
675 program (sponsored by NASA's EOS Validation Pro-  
676 gram). It contributes to the projects CARBODATA  
677 and CARBOEUROFLUX of the European Union  
678 (supported by the EC's Fifth Framework Program,  
679 R&TD contract CARBOEUROFLUX, contract no.  
680 EVK2-CT-1999-0032), and the AmeriFlux program  
681 (US Department of Energy's Terrestrial Carbon Pro-  
682 gram, and NIGEC Program).

## Appendix A

683  
684 Estimates of  $F_{GPP}$  depend crucially on the quality  
685 of derived  $F_{RE}$  values, as  $F_{GPP}$  is calculated as the sum  
686 of  $F_{RE}$  and measured  $F_{NEP}$ . Apparently, the deriva-  
687 tion of  $F_{RE}$  and the quality of the fit of Eq. (1) to  
688 night-time fluxes of  $F_{NEP}$  is critical to all the results  
689 and conclusions presented in this paper. During data  
690 processing ca. 36,000 of such fits were performed, 335  
691 fits for each of 103 site-years (335 running periods  
692 of 30-days; for more information, see Section 2). For  
693 illustration, Table 4 lists minimum, maximum, aver-  
694 age and standard deviation (S.D.) of the 335  $R^2$ -values  
695 of one-third of the available site-years. Comparing  
696 the average  $R^2$  and S.D. of all 103 site-years reveals  
697 that maritime/Mediterranean systems and coniferous  
698 forests show the largest average ( $R^2 = 0.73$  and  $0.72$ ).  
699 Deciduous forests and grasslands have intermediate  
700 values of average  $R^2 = 0.65$  and  $0.70$ , respectively.  
701 Lowest average  $R^2$  of 0.61 are found for the crop-  
702 land sites, indicating that the confidence in derived  
703  $F_{RE}$  values decreases in the order evergreen forest >  
704 deciduous forest > grassland > crop sites. In addi-  
705 tion, the seasonal variation in  $R^2$  increases in more or  
706 less the same order, indicated by the average standard  
707 deviation of  $F_{RE}$  values within those groups, 0.08 for  
708 the maritime/Mediterranean sites, 0.14 for coniferous  
709 forest sites, 0.15 for deciduous forest sites, 0.23 for  
710 grasslands, and 0.22 for crops. Especially for the lat-  
711 ter the seasonal values of  $R^2$  were quite variable: peri-  
712 ods where  $R^2$  dropped below 0.2 coincided, e.g. with  
713 non-vegetated periods for crops, or temperatures be-  
714 low freezing. Yet during those periods overall respira-  
715 tion rates are expected to be quite low, so that eventual  
716 errors due to the low quality of the fit are small, and  
717 we decided to keep the respective  $F_{RE}$  estimates to  
718 calculate monthly and annual sums of  $F_{RE}$  and  $F_{GPP}$ .

## References

- 719  
720 Alward, R.D., Detling, J.K., Milchunas, D.G., 1999. Grassland  
721 vegetation changes and nocturnal global warming. *Science* 283,  
722 229–231.  
723 Amiro, B.D., 2001. Paired-tower measurements of carbon and  
724 energy fluxes following disturbance in the boreal forest. *Global*  
725 *Change Biol.* 7, 253–268.  
726 Aubinet, M., Grelle, A., Ibrom, A., Rannik, Ü., Moncrieff,  
727 J., Foken, T., Kowalski, A.S., Martin, P.H., Berbigier, P.,

- 728 Bernhofer, Ch., Clement, R., Elbers, J., Granier, A., Grünwald,  
729 T., Morgenstern, K., Pilegaard, K., Rebmann, C., Snijders,  
730 W., Valentini, R., Vesala, T., 2000. Estimates of the annual  
731 net carbon and water exchange of forests: the EUROFLUX  
732 methodology. *Adv. Ecol. Res.* 30, 113–175.
- 733 Baldocchi, D.D., Finnigan, J., Wilson, K., Paw U, K.T., Falge, E.,  
734 2000. On measuring net ecosystem carbon exchange over tall  
735 vegetation on complex terrain. *Boundary Layer Meteorol.* 96,  
736 257–291.
- 737 Baldocchi, D., Falge, E., Wilson, K., 2001. A spectral  
738 analysis of biosphere-atmosphere trace gas flux densities and  
739 meteorological variables across hour to multi-year time scales.  
740 *Agric. For. Meteorol.* 107, 1–27.
- 741 Bergen, K., Dobson, M.C., 1999. Integration of remotely sensed  
742 radar imagery in modeling and mapping of forest biomass and  
743 net primary production. *Ecol. Modell.* 122, 257–274.
- 744 Black, T.A., den Hartog, G., Neumann, H.H., Blanken, P.D., Yang,  
745 P.C., Russell, C., Nescic, Z., Lee, X., Chen, S.G., Staebler, R.,  
746 Novak, M.D., 1996. Annual cycles of water vapour and carbon  
747 dioxide fluxes in and above a boreal aspen forest. *Global Change*  
748 *Biol.* 2, 101–111.
- 749 Black, T.A., Chen, W.J., Barr, A.G., Arain, M.A., Chen, Z., Nescic,  
750 Z., Hogg, E.H., Neumann, H.H., Yang, P.C., 2000. Increased  
751 carbon sequestration by a boreal deciduous forest in years with  
752 a warm spring. *Geophys. Res. Lett.* 27, 1271–1274.
- 753 Ciais, P., Friedlingstein, P., Schimel, D.S., Tans, P.P., 1999. A  
754 global calculation of the delta C-13 of soil respired carbon:  
755 implications for the biospheric uptake of anthropogenic CO<sub>2</sub>.  
756 *Global Biogeochem. Cy.* 13 (2), 519–530.
- 757 Cramer, W., Kicklighter, D.W., Bondeau, A., Moore, III, B.,  
758 Churkina, G., Nemry, B., Ruimy, A., Schloss, A.L., The  
759 Participants of the Potsdam NPP Model Intercomparison, 1999.  
760 Comparing global models of terrestrial net primary productivity  
761 (NPP): overview and key results. *Global Change Biol.* 5  
762 (Suppl.), 1–15.
- 763 Davidson, E.A., Belk, E., Boone, R.D., 1998. Soil water  
764 content and temperature as independent or confounded factors  
765 controlling soil respiration in a temperate mixed hardwood  
766 forest. *Global Change Biol.* 4, 217–227.
- 767 Easterling, D.R., Horton, B., Jones, P.D., Peterson, T.C., Karl,  
768 T.R., Parker, D.E., Salinger, M.J., Razuvayev, V., Plummer,  
769 N., Jamason, P., Folland, C.K., 1997. Maximum and minimum  
770 temperature trends for the globe. *Science* 277, 364–367.
- 771 Edwards, N.T., 1975. Effects of temperature and moisture on  
772 carbon dioxide evolution in a mixed deciduous forest floor. *Soil*  
773 *Sci. Soc. Am. Proc.* 39, 361–365.
- 774 Falge, E., Baldocchi, D., Olson, R.J., Anthoni, P., Aubinet, M.,  
775 Bernhofer, C., Burba, G., Ceulemans, R., Clement, R., Dolman,  
776 H., Granier, A., Gross, P., Grünwald, T., Hollinger, D., Jensen,  
777 N.-O., Katul, G., Keronen, P., Kowalski, A., Ta Lai, C., Law,  
778 B.E., Meyers, T., Moncrieff, J., Moors, E., Munger, J.W.,  
779 Pilegaard, K., Rannik, Ü., Rebmann, C., Suyker, A., Tenhunen,  
780 J., Tu, K., Verma, S., Vesala, T., Wilson, K., Wofsy, S.,  
781 2001. Gap filling strategies for defensible annual sums of net  
782 ecosystem exchange. *Agric. Meteorol.* 107, 43–69.
- 783 Falge, E., Tenhunen, J.D., Baldocchi, D.D., et al., 2002. Phase and  
784 amplitude of ecosystem carbon release and uptake potentials as  
derived from FLUXNET measurements. *Agric. For. Meteorol.*, 785  
submitted for publication. 786
- Fan, S., Gloor, M., Mahlman, J., Pacala, S., Sarmiento, J.,  
787 Takahashi, T., Tans, P., 1998. A large terrestrial carbon sink  
788 in North America implied by atmospheric and oceanic carbon  
789 dioxide data and models. *Science* 282, 442–446. 790
- Field, C.B., Randerson, J.T., Malmström, C.M., 1995. Global net  
791 primary production: combining ecology and remote sensing.  
792 *Remote Sens. Environ.* 51, 74–88. 793
- Field, C.B., Behrenfeld, M.J., Randerson, J.T., Falkowski, P., 1998.  
794 Primary production of the biosphere: integrating terrestrial and  
795 oceanic components. *Science* 281, 237–240. 796
- Fliebach, A., Sarig, S., Steinberger, Y., 1994. Effects of water  
797 pulses and climatic conditions on microbial biomass kinetics  
798 and microbial activity in a Yermosol of the central Negev. *Arid*  
799 *Soil Res. Rehab.* 8, 353–362. 800
- Friedlingstein, P., Fung, I., Holland, E., John, J., Brasseur, G.,  
801 Erickson, D., Schimel, D., 1995. On the contribution of CO<sub>2</sub>  
802 fertilization to the missing biospheric sink. *Global Biogeochem.*  
803 *Cy.* 9 (4), 541–556. 804
- Goetz, S.J., Prince, S.D., Goward, S.N., Thawley, M.M., Small,  
805 J., 1999. Satellite remote sensing of primary production:  
806 an improved production efficiency modeling approach. *Ecol.*  
807 *Modell.* 122, 239–255. 808
- Goulden, M.L., Munger, J.W., Fan, S.M., Daube, B.C., Wofsy,  
809 S.C., 1996. Measurement of carbon storage by long-term eddy  
810 correlation: methods and a critical assessment of accuracy.  
811 *Global Change Biol.* 2, 169–182. 812
- Goulden, M.L., Wofsy, S.C., Harden, J.W., Trumbore, S.E., Crill,  
813 P.M., Gower, S.T., Fries, T., Daube, B.C., Fan, S.M., Sutton,  
814 D.J., Bazzaz, A., Munger, J.W., 1998. Sensitivity of boreal  
815 forest carbon balance to soil thaw. *Science* 279, 214–217. 816
- Hanson, P.J., Wullschleger, S.D., Bohlman, S.A., Todd, D.E., 1993.  
817 Seasonal and topographic patterns of forest floor CO<sub>2</sub> efflux  
818 from an upland oak forest. *Tree Physiol.* 13, 1–15. 819
- Hasenauer, H., Nemani, R.R., Schadauer, K., Running, S.W., 1999.  
820 Forest growth response to changing climate between 1961 and  
821 1990 in Austria. *For. Ecol. Manage.* 122, 209–219. 822
- Houghton, J.T., Meira Filho, L.G., Callander, B.A., Harris, N.,  
823 Kattenberg, A., Maskell, K. (Eds.), 1996. *Climate Change*  
824 *1995—The Science of Climate Change.* Cambridge University  
825 Press, Cambridge. 826
- Jackson, R.B., Lechowicz, M.J., Li, X., Mooney, H.A., 2000.  
827 The roles of phenology, growth, and allocation in global  
828 terrestrial productivity. In: Mooney, H.A., Saugier, B., Roy, J.  
829 (Eds.), *Terrestrial Global Productivity: Past, Present, and Future.*  
830 Academic Press, San Diego, pp. 61–82. 831
- Janssen, I.A., Lankreijer, H., Matteucci, G., Kowalski, A.S.,  
832 Buchmann, N., Epron, D., Pilegaard, K., Kutsch, W., Longdoz,  
833 B., Grünwald, T., Montagnani, L., Dore, S., Rebmann, C.,  
834 Moors, E.J., Grelle, A., Rannik, Ü., Morgenstern, K., Oltchev,  
835 S., Clement, R., Guðmundsson, J., Minerbi, S., Berbigier, P.,  
836 Ibrom, A., Moncrieff, J., Aubinet, M., Bernhofer, C., Jensen,  
837 N.-O., Vesala, T., Granier, A., Schulze, E.-D., Lindroth, A.,  
838 Dolman, A.J., Jarvis, P.G., Ceulemans, R., Valentini, R., 2001.  
839 Productivity overshadows temperature in determining soil and  
840 ecosystem respiration across European forests. *Global Change*  
841 *Biol.* 7, 269–278. 842

- 843 Jiang, H., Apps, M.J., Zhang, Y., Peng, Ch., Woodward, P.M.,  
844 1999. Modelling the spatial pattern of net primary productivity  
845 in Chinese forests. *Ecol. Modell.* 122, 275–288.
- 846 Keeling, C.D., Chin, J.F.S., Whorf, T.P., 1996a. Increased  
847 activity of northern vegetation inferred from atmospheric CO<sub>2</sub>  
848 observations. *Nature* 382, 146–149.
- 849 Keeling, R.F., Piper, S.C., Heimann, M., 1996b. Global and  
850 hemispheric CO<sub>2</sub> sinks deduced from changes in atmospheric  
851 O<sub>2</sub> concentration. *Nature* 381, 218–221.
- 852 Keyser, A.R., Kimball, J.S., Nemani, R.R., Running, S.W., 2000.  
853 Simulating the effects of climate change in the carbon balance  
854 of North American high-latitude forests. *Global Change Biol.*  
855 6, 185–195.
- 856 Kohlmaier, G.H., Badeck, F.-W., Otto, R.D., Häger, C., Dönges,  
857 S., Kindermann, J., Würth, G., Lang, T., Jäkel, U., Nadler,  
858 A., Ramge, P., Klaudius, A., Habermehl, S., Lüdeke, M.K.B.,  
859 1997. The Frankfurt Biosphere Model: a global process-oriented  
860 model for the seasonal and long-term CO<sub>2</sub> exchange between  
861 terrestrial ecosystems and the atmosphere. II. Global results for  
862 potential vegetation in an assumed equilibrium state. *Climate*  
863 *Res.* 8, 61–87.
- 864 Law, B.E., Ryan, M.G., Anthoni, P.M., 1999. Seasonal and annual  
865 respiration of a Ponderosa pine ecosystem. *Global Change Biol.*  
866 5 (1), 69–182.
- 867 Law, B., Williams, M., Anthoni, P., Baldocchi, D.D., Unsworth,  
868 M.H., 2000. Measuring and modeling seasonal variation of  
869 carbon dioxide and water vapor exchange of a *Pinus ponderosa*  
870 forest subject to soil water deficit. *Global Change Biol.* 6, 613–  
871 630.
- 872 Lee, X., 1998. On micrometeorological observations of surface-air  
873 exchange over tall vegetation. *Agric. Meteorol.* 91, 39–50.
- 874 Lieth, H.F.H., 1975. Primary production of the major vegetation  
875 units of the world. In: Lieth, H., Whittaker, R.H. (Eds.), *Primary*  
876 *Productivity of the Biosphere: Ecological Studies*, Vol. 14.  
877 Springer, Berlin, pp. 203–215.
- 878 Lloyd, J., Taylor, J.A., 1994. On the temperature dependence of  
879 soil respiration. *Funct. Ecol.* 8, 315–323.
- 880 Menzel, A., Fabian, P., 1999. Growing season extended in Europe.  
881 *Nature* 397, 659.
- 882 Meyers, T., in press. A comparison of summertime water and CO<sub>2</sub>  
883 fluxes over rangeland for well watered and drought conditions,  
884 *Agric. Meteorol.*
- 885 Moncrieff, J.B., Mahli, Y., Leuning, R., 1996. The propagation of  
886 errors in long term measurements of land atmosphere fluxes of  
887 carbon and water. *Global Change Biol.* 2, 231–240.
- 888 Myneni, R.B., Keeling, C.D., Tucker, C.J., Asrar, G., Nemani,  
889 R.R., 1997. Increased plant growth in the northern high latitudes  
890 from 1981 to 1991. *Nature* 386, 698–702.
- 891 Nemry, B., François, L., Gérard, J.-C., Bondeau, A., Heimann, M.,  
892 The Participants of the Potsdam NPP model intercomparison,  
893 1999. Comparing global models of terrestrial net primary  
894 productivity (NPP): analysis of the seasonal atmospheric CO<sub>2</sub>  
895 signal. *Global Change Biol.* 5 (Suppl.), 65–76.
- 896 Raich, J.W., Schlesinger, W.H., 1992. The global carbon dioxide  
897 flux in soil respiration and its relationship to vegetation and  
898 climate. *Tellus B* 44, 81–99.
- 899 Raich, J.W., Tufekciogul, A., 2000. Vegetation and soil respiration:  
900 correlations and controls. *Biogeochemistry* 48 (1), 71–90.
- Randerson, J.T., Field, C.B., Fung, I.Y., Tans, P.P., 1999. Increases 901  
in early season ecosystem uptake explain recent changes in the 902  
seasonal cycle of atmospheric CO<sub>2</sub> at high northern latitudes. 903  
*Geophys. Res. Lett.* 26, 2765–2768. 904
- Rastetter, E.B., McKane, R.B., Shaver, G.R., Melillo, J.M., 1992. 905  
Changes in C storage by terrestrial ecosystems: how C–N 906  
interactions restrict responses to CO<sub>2</sub> and temperature. *Water* 907  
*Air Soil Poll.* 64, 327–344. 908
- Running, S.W., Baldocchi, D.D., Turner, D., Gower, S.T., Bakwin, 909  
P., Hibbard, K., 1999. A global terrestrial monitoring network, 910  
scaling tower fluxes with ecosystem modeling and EOS satellite 911  
data. *Remote Sens. Environ.* 70, 108–127. 912
- Schulze, E.-D., 1982. Plant life forms as related to plant carbon, 913  
water and nutrient relations. In: Lange, O.L., Nobel, P.S., 914  
Osmond, C.B., Ziegler, H. (Eds.), *Encyclopedia of Plant* 915  
*Physiology, Physiological Plant Ecology, Water Relations* 916  
*and Photosynthetic Productivity*, Vol. 12B. Springer, Berlin, 917  
pp. 615–676. 918
- Schulze, E.-D., Lloyd, J., Kelliher, F.M., Wirth, C., Rebmann, C., 919  
Luhker, B., Mund, M., Knohl, A., Milyukova, I.M., Schulze, 920  
W., Ziegler, W., Varlagin, A.B., Sogachev, A.F., Valentini, R., 921  
Dore, S., Grigoriev, S., Kolle, O., Panfyorov, M.I., Tchebakova, 922  
N., Vygodskaya, N.N., 1999. Productivity of forests in the 923  
Eurosiberian boreal region and their potential to act as a carbon 924  
sink—a synthesis. *Global Change Biol.* 5 (6), 703–722. 925
- Sellers, P.J., Randall, D.A., Collatz, G.J., Berry, J.A., Field, C.B., 926  
Dazlich, D.A., Zhang, C., Collelo, G.D., Bounoua, L., 1996a. 927  
A revised land surface parameterization (SiB<sub>2</sub>) for atmospheric 928  
GCMs. Part I. Model formulation. *J. Climatol.* 9, 676–705. 929
- Sellers, P.J., Los, S.O., Tucker, C.J., Justice, C.O., Dazlich, D.A., 930  
Collatz, G.J., Randall, D.A., 1996b. A revised land surface 931  
parameterization (SiB<sub>2</sub>) for atmospheric GCMs. Part II. The 932  
generation of global fields of terrestrial biophysical parameters 933  
from satellite data. *J. Climatol.* 9, 706–737. 934
- Suyker, A.E., Verma, Sh.B., 2001. Year-round observations of the 935  
net ecosystem exchange of carbon dioxide in a native tall grass 936  
prairie. *Global Change Biol.* 7, 279–289. 937
- Tans, P.P., Fung, I.Y., Takahashi, T., 1990. Observational 938  
constraints on the global atmospheric CO<sub>2</sub> budget. *Science* 247, 939  
1431–1438. 940
- Valentini, R. (Ed.), 2000. The Euroflux dataset 2000. In: *Carbon,* 941  
*Water and Energy Exchanges of European Forests*. Springer, 942  
Heidelberg, p. 300. 943
- Valentini, R., Matteucci, G., Dolman, A.J., Schulze, E.-D., 944  
Rebmann, C., Moors, E.J., Granier, A., Gross, P., Jensen, N.-O., 945  
Pilegaard, K., Lindroth, A., Grelle, A., Bernhofer, C., Grünwald, 946  
T., Aubinet, M., Ceulemans, R., Kowalski, A.S., Vesala, T., 947  
Rannik, U., Berbigier, P., Loustau, D., Guðmundsson, J., 948  
Thorgeirsson, H., Ibrom, A., Morgenstern, K., Clement, R., 949  
Moncrieff, J., Montagnani, L., Minerbi, S., Jarvis, P., 2000. 950  
Respiration as the main determinant of carbon balance in 951  
European forests. *Nature* 404, 861–865. 952
- Walker, B.H., Steffen, W.L., Langridge, J., 1999. Interactive and 953  
integrated effects of global change on terrestrial ecosystems. 954  
In: Walker, B.H., Steffen, W.L., Canadell, J., Ingram, J.S.I. 955  
(Eds.), *Implications of Global Change for Natural and Managed* 956  
*Ecosystems: A Synthesis of GCTE and Related Research.* 957

- 958 International Geosphere–Biosphere Programme (IGBP) Book  
959 Series No. 4, Cambridge University Press, Cambridge, UK.
- 960 Waring, R.H., Schlesinger, W.H., 1985. Forest Ecosystems:  
961 Concepts and Management. Academic Press, San Diego, CA,  
962 pp. 263–276.
- 963 Warnant, P., Francois, L., Strivay, D., Gerard, J.-C., 1994.  
964 CARAIB: a global model of terrestrial biological productivity.  
965 Global Biogeochem. Cy. 8, 255–270.
- 966 White, M.A., Running, S.W., Thornton, P.E., 1999. The impact of  
967 growing-season length variability on carbon assimilation and  
968 evapotranspiration over 88 years in the eastern US deciduous  
forest. *Int. J. Biometeorol.* 42, 139–145. 969
- Xu, M., Qi, Y., in press. Soil surface CO<sub>2</sub> efflux and its spatial  
and temporal variations in a young Ponderosa pine plantation  
in northern California. *Global Change Biol.* 970  
971 972
- Xu, M., DeBiase, T., Qi, Y., Goldstein, A., Liu, Z., 2001. 973  
Ecosystem respiration in a young Ponderosa pine plantation  
in the Sierra Nevada Mountains, California. *Tree Physiol.* 21, 974  
309–318. 975  
976  
977